Supplementary material

Biotic interactions may be more important than climate for shaping animal niches

1. Changing landscapes during deglaciation

During deglaciation, there were changes in glacial ice extent [1,2], sea level [3,4], and the size of ice-dammed lakes [5] in northern Fennoscandia. When these factors are combined, it becomes clear how the landscape formed a mosaic of dispersal barriers and highways for different organisms. For some species, like geese and freshwater plants and invertebrates, the large ice-dammed lakes that temporarily formed during ice melt may have represented dispersal highways while they at the same time represented dispersal barriers to terrestrial mammals.

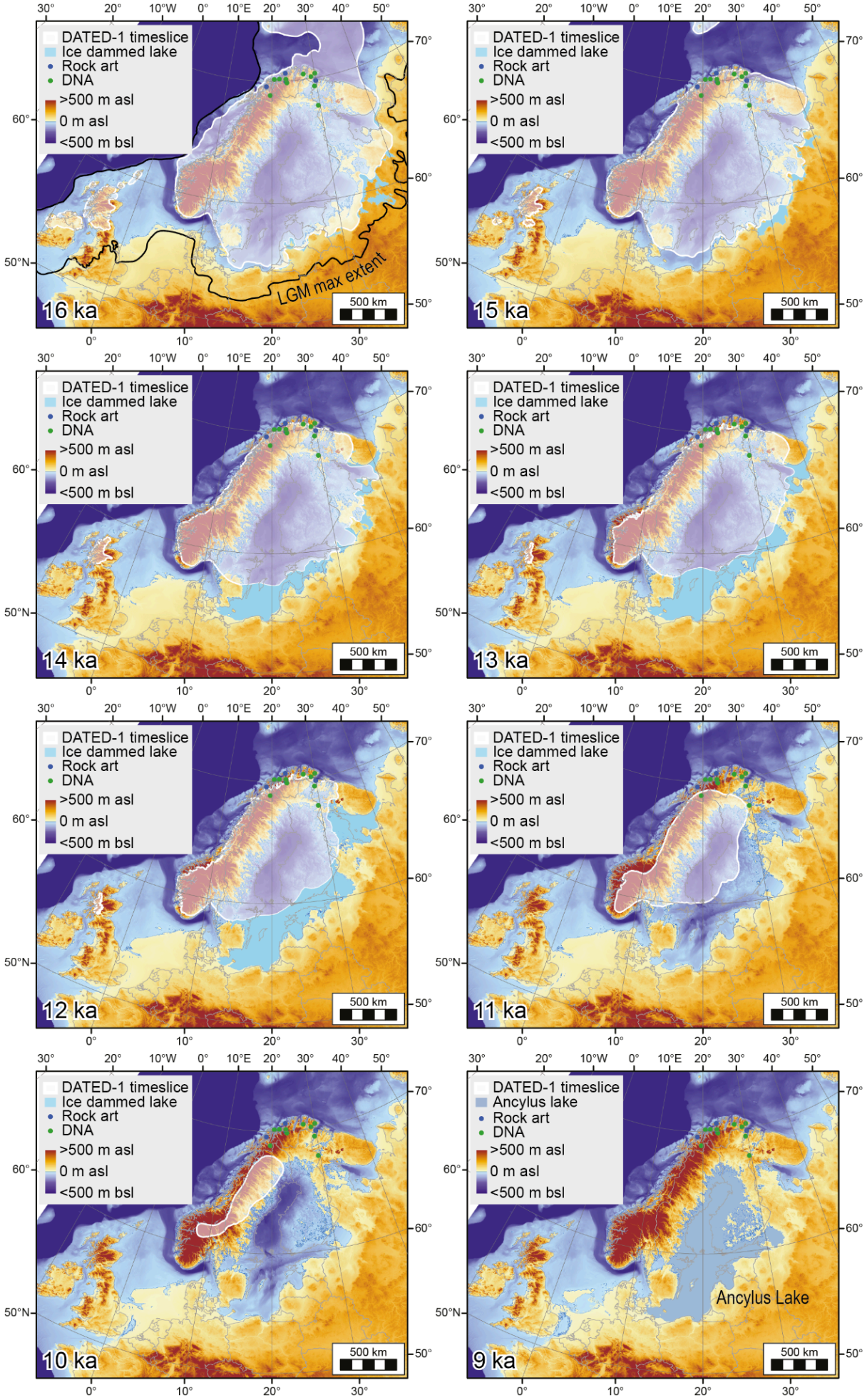
DATED-1 timeslice
Ice dammed lake
Rock art
DNA
>500 m asl
0 m asl
<500 m bsl
LGM max extent
16 ka
15 ka
14 ka
13 ka
12 ka
11 ka
10 ka
Ancylus lake
Ancylus Lake
9 ka
500 km

Supplementary Fig. 1.1 sedaDNA coring sites and rock art sites in relation to the glacio-isostatically modelled palaeo-topography [6], most-credible ice-sheet extent [1], and predicted paleo-shorelines determining the extent and position of ice-dammed lakes and marine sectors, for one thousand year time slices between 16 and 9 ka.

2. Catchments and taphonomy

2.1 The theory

The fate of DNA from deposition to sediments is shown in Fig. S2.1. The source of plant, mammal and much invertebrate sedaDNA is the soil and slopes of the hydrological catchment of the lake [7–10]. After cell lysis during decomposition of litter and below ground biomass (e.g. roots), DNA is released into the pore waters of the soil [11]. This DNA has a half-life in aqueous solution of minutes to a few hours if not protected from UV light, temperature and nucleases in the microbial environment (Collins et al. 2018). However, a small proportion is protected from further fragmentation by being adsorbed onto minerals, particularly clays, and organic complexes [12,13]. Some clays can even incorporate DNA strands into their structure (nanoconfinement) and be preserved for two million years [14]. These mineral and organic particles are then transported by overland water flow with their adsorbed DNA to streams and rivers and then into lakes, estuaries or coastal areas [7,15]. Because the DNA is attached preferentially to the finer part of the suspended river load it is carried out into the lake and settles out with decreasing thickness away from the river input. In small-medium sized lakes of shallow to moderate depth (4-30m) this fine layer is minimally disturbed although micro-scale bioturbation can be caused by seasonal resuspension, wave action (down to c. 4m) and micro-bioturbation by benthic fauna such as tubificid worms. This will cause mm to a few cm of mixing and depending upon the accumulation rate may blur the resultant age model by a few years. Where this does not occur, annual laminations (pseudo-varves) can be preserved along with flood layers caused by larger floods, which are routinely used to create flood chronologies [16]. This has been validated by sedaDNA which reflects a larger source area within the catchment than between the floods reflecting the expansion of ‘contributing area’ of sediment for larger hydrological events [17]. Thousands of studies of lake sediment fabric (3D arrangement of particles) have revealed that the movement of clay and fine organic matter does not occur in lakes sediment columns due to saturation of pore water spaces and a lack of hydraulic gradient. Lake sediments can be disturbed where bed slopes are steep causing sediment focusing and if currents or channels erode into the lake floor producing problems particularly on larger and more bathymetrically complex lakes. However, in small shallow single basin lakes, the sediment column preserves a faithful record of changes over time in sediment mineralogy, geochemistry, microfossils and organic molecules bound to mineral and organic particles with no vertical mixing. This can even be validated from *sed*aDNA which record to within a few years changes in catchment vegetation or known introductions [18,19].

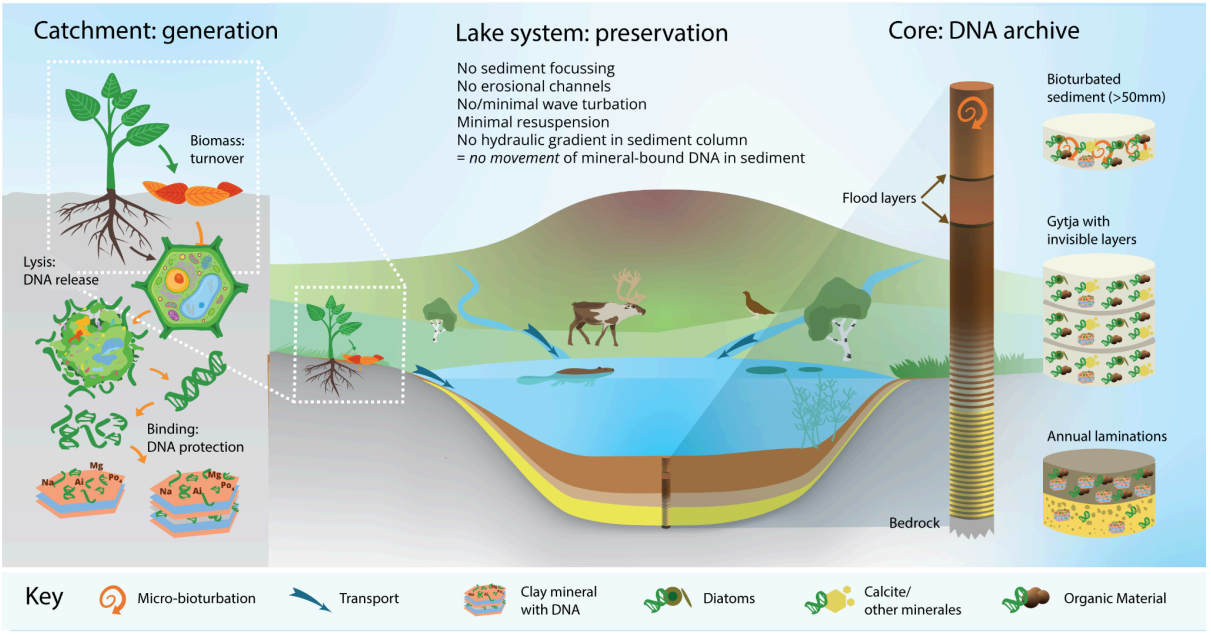

Supplementary Fig 2.1. Catchment sources of DNA and its deposition in lake sediments. Left panel: Upon cell lysis, DNA is released and a small fraction bound to organic and mineral partcles, especially clays. Central panel: Particles with DNA are transported by overland flow and streams to be depositied on lake floors. Right panet: The sediment column showing the sequential deposition of DNA, here shown as a transition from clastic dominated warved (annual laminated) to organic dominated (gytja) sediments with flood layers. Microbioturbation in top sediment may cause mixing of a few centimetre. By selecting morphologically simple lakes where there is no sediment erosion and re-deposition, the DNA is stratified in a reliable time sequence.

2.2 Our application

The catchments used in this study were chosen specifically so that taphonomic variation and complicating factors would be minimized following both our recent taphonomic studies [8] and work elsewhere [7,20]. So all our lakes were small (Table S1) being <60 ha (and mostly under 15 ha) and shallow (under 15 m except for one), with simple bathymetry and gentle sediment surface slopes, negating any sediment-focussing effects. The lake catchments were also small with all except one being under 11 km^2. Additionally, most of the lakes were also in headwater catchments with no upstream lake inputs and all except one (Sandfjordalen) had no significant upstream floodplains or areas of colluvial sediment storage. That we do not have eroded *sed*aDNA is supported by a lack of any out-of sequence taxa or indeed taxa from previous warm-periods. The lakes are also dominated by in-lake organic production with relatively stable levels of mineral input except in the pre-Holocene (see XRF, Supplementary Fig. S2.2; For Kuutsjävri see [21]). Whilst Al is present in all cores, reflecting clays, it varies being low in sections with marine sands in Langfjordvannet and high in periods of fine marine sedimentation in Nordivatnet, whereas it is intermediate in all lacustrine sections. These results suggest adequate clay content in all sediments for the unbiased preservation of sedaDNA. Only two lakes have significant change in carbonate component in the early Holocene (Fig S2.2) and virtually no mineral in-wash bands were

seen, although the Si and Ti record of Langfjordvannet reflects sand inwashes. Otherwise, a lack of inwashes of silt-clay-organic matter and reworking is also supported by under 10 ^{14}C date reversals, with only 5 being older dates (i.e. possible unwashed organic matter) out of over 120 dates in the Holocene [22], with 5 of these coming from two sites (Sandfjordalen and Sierrevatnet, Supplementary Fig. 2.2). This is unlike the records from lakes in most other areas of Europe [7] and reflects the lack of agriculture in these catchments [23]. The result is that the input of *sed*aDNA to the lake was by continuous stream and lake-edge transfer and so would have reflected the presence of the taxa rather than a delayed response due to temporal sediment dynamics. Lastly, the lakes all share the same or similar geologies (metamorphic gneiss, schists and slates) which produce the same suit of clay minerals that include some swelling clays which have a high affinity to sedaDNA [24]. thus, the cores can be regarded as cumulative records as there is abundant evidence now that *sed*aDNA cannot be leached from one level to another in saturated lake sediments [18] – as also applies to other biomarkers and geochemistry. In this sedimentary context, DNA damage patterns are not required for ancient DNA authentication, and *sed*aDNA metabarcoding data are regarded as reliable source of chronological ecosystem changes [25–27].

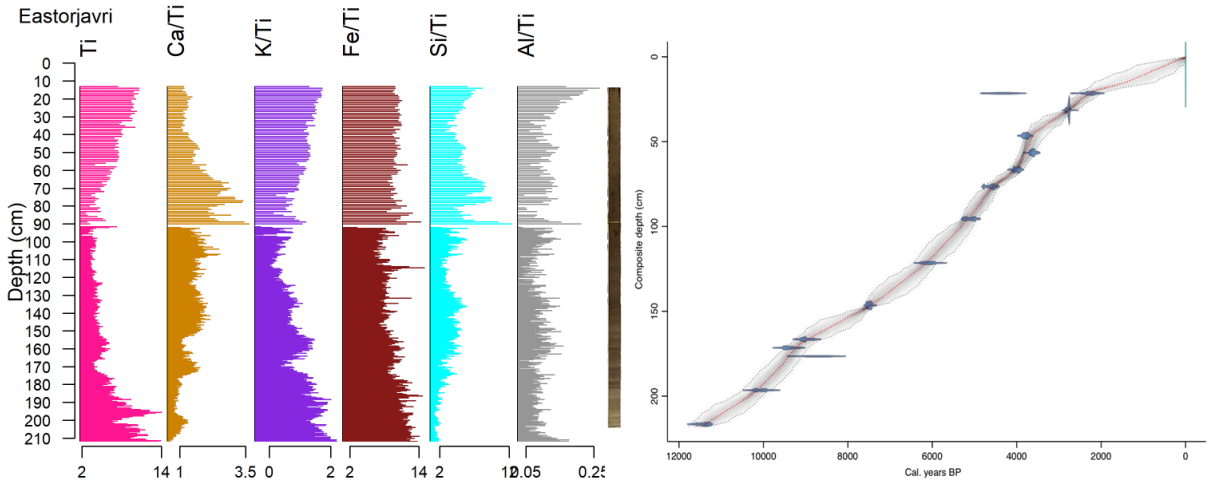

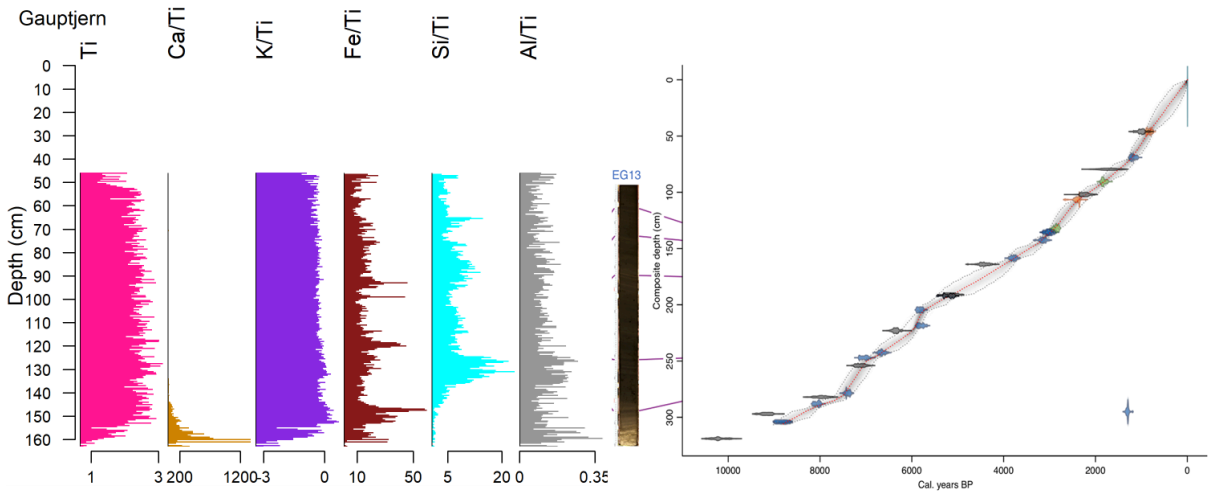

134

135

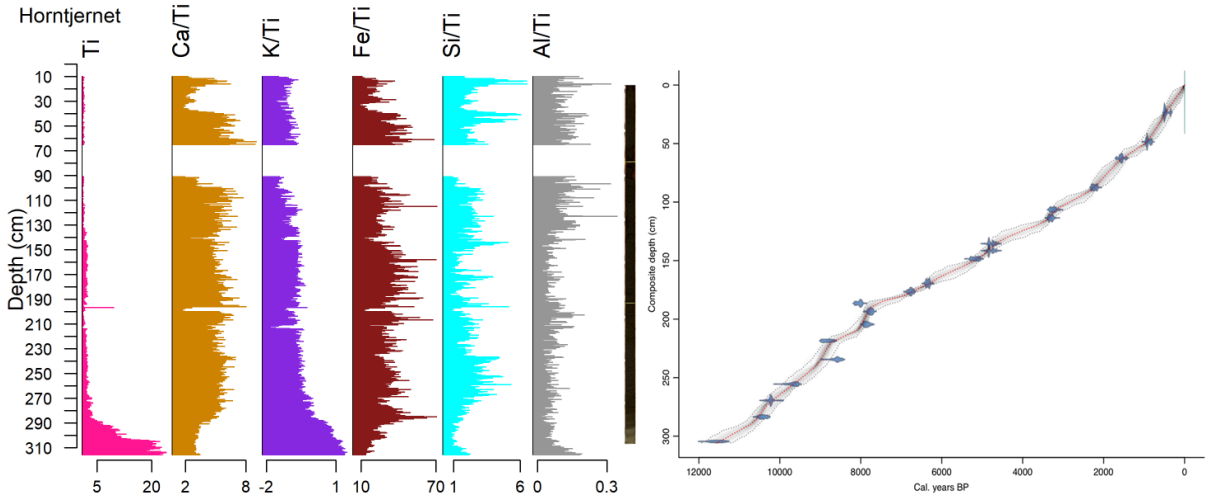

136

137

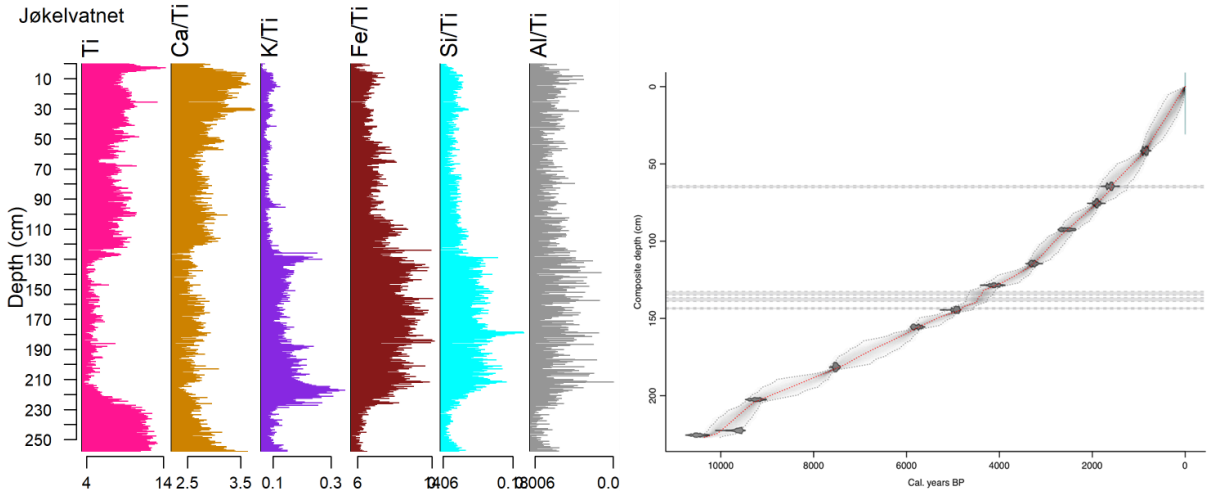

138

139

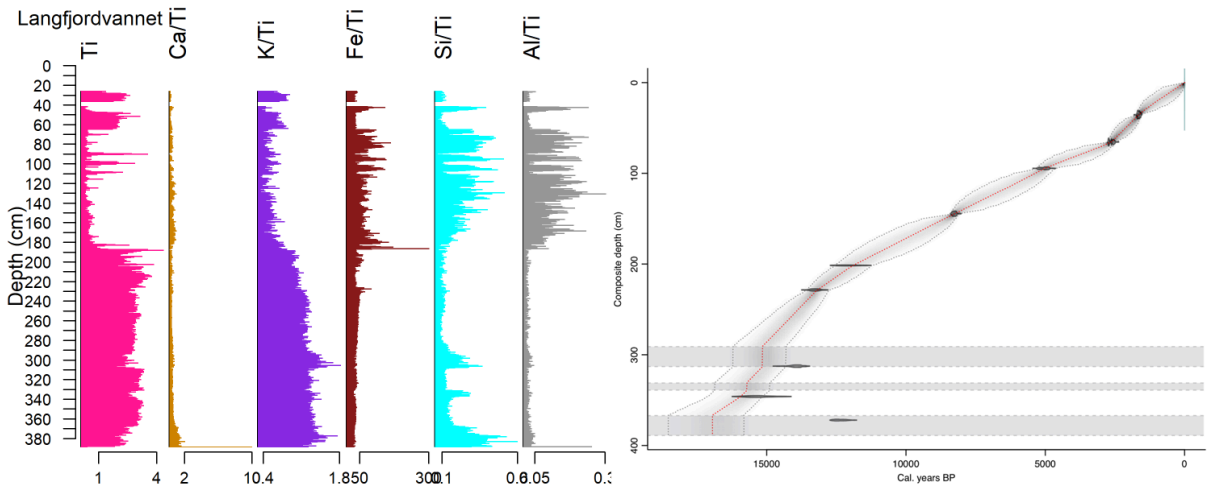

140

141

142

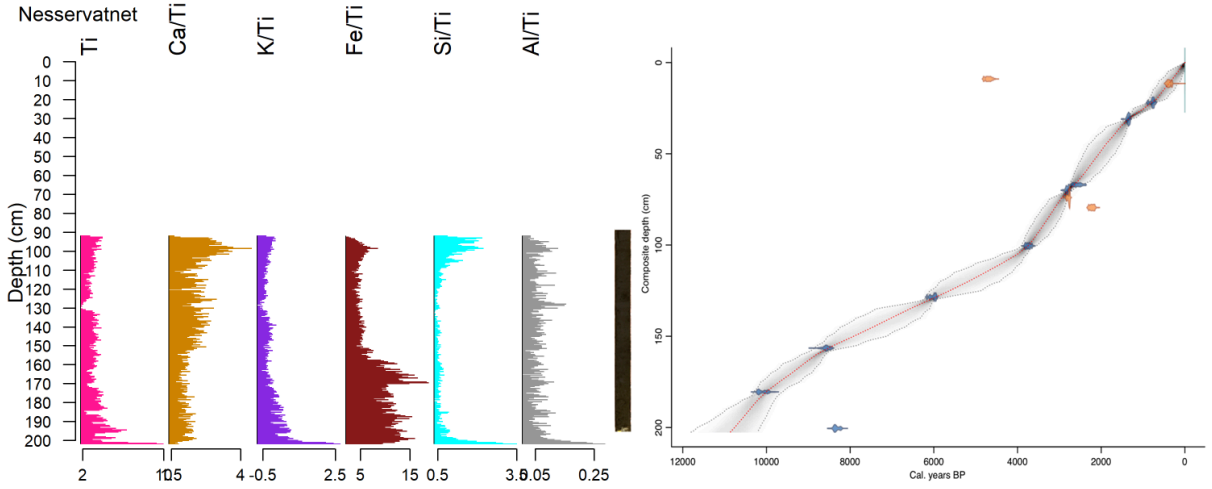

143

144

145

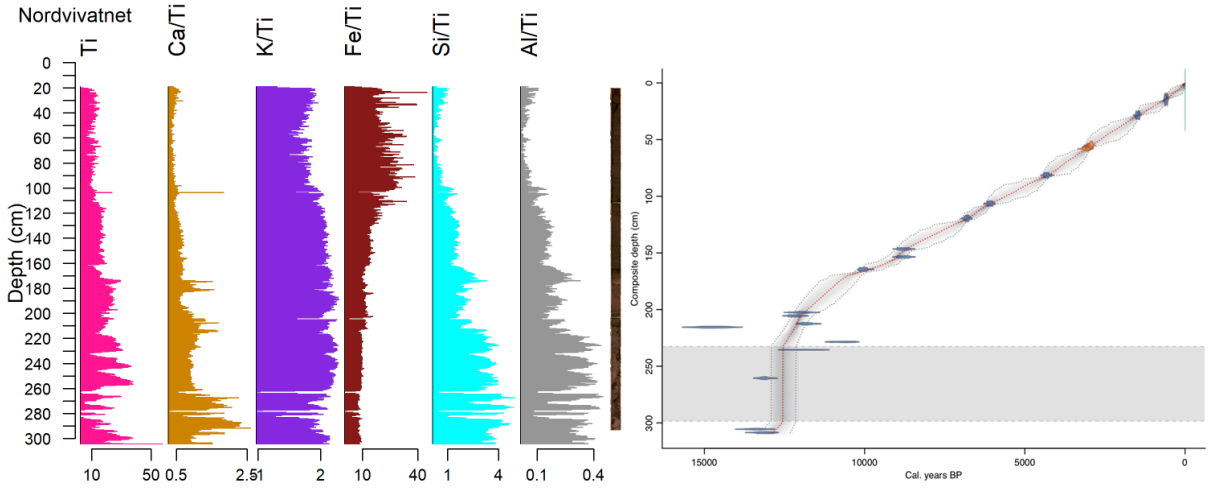

146

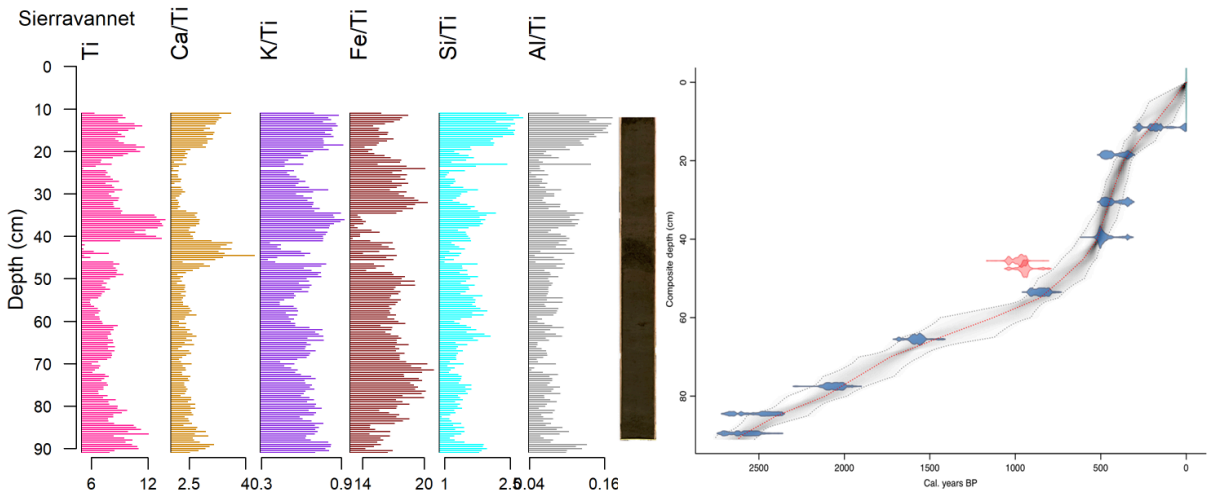

Supplementary Fig. 2.2: Selected elements from XRF analysis and age-depth model for Sierravannet (EG07). Raw counts of all other elements were divided by Titanium (Ti) and raw counts and Ti itself was rescaled by dividing it by 1000. Unusual high values were removed assuming core start and core breaks. This regards for 12 and 91 cm depths for Eastorjavri; 162 cm depth for Gauptjern; and 110, 186.5 and 389 cm for Langfjordvannet. Age-deth models are taken from [22] with minor updates from [28]. Full XRF dataset is given as Supplementary Data 1.

3. Mitigating false positives from sampling to final dataset

To minimize the risk of false positives, we took necessary steps all along the process from coring to the final stage of bioinformatic and manual cross-checking of the data. During coring, DNA from the environment may potentially enter the sediments. To avoid this, we used a closed coring system like Nesje corer [29]. Before coring, we smeared/spread the pipe, piston and core head with extracted plant DNA of a Christmas cactus (*Schlumbergera truncata* cultivar) (Supplementary Fig. 3.1a), which belongs to a plant family (Cactaceae) not native to Eurasia. DNA from the same plant was also genome skimmed as part of PhyloNorway, and we have never recorded it in any of our *sed*aDNA data, suggesting that contamination during the field in general is of low risk.

During core splitting and sampling, as well as DNA extraction, all procedures are carried out sequentially from the oldest to the youngest sediment layers to prevent contamination of older layers by younger ones. Consequently, if cross-contamination were to occur during laboratory processing, it would more likely be from the older sediments to the younger ones.

All ancient DNA work is done in a dedicated lab for ancient DNA with over pressure. All personnel working in the lab are wearing fully body suits and masks. In addition, specific lab clothes that are not worn outside are used underneath the suits. All items brought into the lab are washed minimum twice with a bleach solution, in addition no outer packaging e.g. cardboard boxes of consumables are entering the inner lab space. This to avoid potential modern contamination.

We cut the plastic of the pipe using a saw, only penetrating 0-1 mm into the 10 cm diameter core. Then we cleaned the pipe with bleach before taking it into the ancient DNA clean laboratory where we split the cores by pulling a string through the core from the oldest to the youngest end of the core. The splitting process risks dragging DNA from the core end and/or the inner core from the older to the younger sediment. Any such contamination is removed by scraping off the upper sediments first once, and then a second time within the first scrape to ensure that only undisturbed sediments are sampled (Supplementary Fig. 3.1b). In addition, a container with DNA free water is placed next to the sampling to monitor any contamination from the DNA lab.

During DNA extraction, a negative control is added at the end of each batch (Supplementary Fig. 3.1c). This is a completely empty sample as no water is added, just controlling for cross-contamination as well as the contamination from reagents as these are not produced for ancient DNA and commonly contain a small amount of DNA from human and domestic species [30,31].

After extraction the samples were randomly placed on a 96 well plate for easier processing for PCR. During the transfer of 85ul DNA extracts from the individual tubes to the plate, a negative control with molecular grade water was added to account for this step. During PCR another negative control is added. In addition, we included the negative controls from sampling and extraction (Supplementary Fig. 3.1d). By including these negative controls at all stages of the process, we can monitor not only which species may occur as contaminants, but also at which stage they entered the process. We did record contamination of chicken (1 negative control) cow (1 negative and 1 positive control), pig (2 negative and 1 positive controls) and human (36 negative controls and 11 positive controls) (Supplementary Data 1). These are common contaminants found in samples analysed in different ancient DNA laboratories [31–33] and are assumed to come from the reagents and/or disposables. It is possible to distinguish this type of modern contamination from ancient DNA by doing shotgun analyses followed by analyses of DNA damage patterns [34]. However, domestic animals were not the focus of this study, and the only species recorded were misidentification between a domestic and wild animal is possible wolf/dog. As carnivores in general occur in low number of reads (mean 24 reads in 60 samples, and damage pattern only found in 8 samples, [32]), we did not attepmt shotgun sequencing to confirm potential wolf occurrence. None of the 85

native animal taxa were detected in any of the 89 controls, supporting no physical contamination of samples.

To avoid cross-over during PCR, we used dual tagging of 8-9 bases (Supplementary Fig. 3.1e). Similarly, to avoid tag jumping during sequencing [35], we used dual tagged library (Supplementary Fig. 3.1f). Thus, the chance that we infer the wrong date of a record due to tag jumping is low.

We matched the DNA sequences to the EMBL standard reference database (downloaded on 2022-10-06) which was manually curated in order to remove erroneously identified sequences. Finally, we evaluated the identified metabarcode dataset manually and removed one sequence that we were not 100% sure if it represented a wolf or contamination from dog DNA.

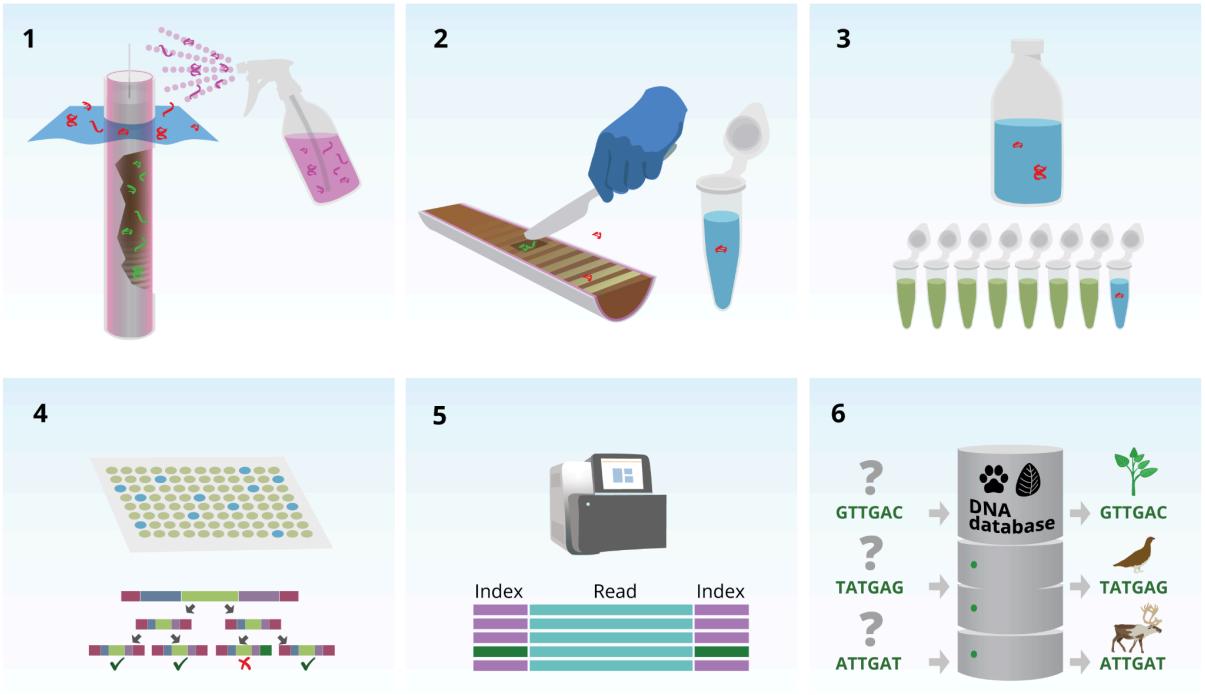

Supplementary Fig. 3. Avoiding false positives in metabarcoding at all steps from sampling to the final dataset. 1) Adding DNA tracer to equipment at coring, 2) Sampling from inner surface after double cleaning; putting out negative control next to sampling to record any background DNA in the clean laboratory, 3) Negative control of DNA-free water at the end of each batch during DNA extraction to record any cross-contamination from samples as well as background DNA from the reagents, 4) Negative controls during PCR as in step 3; dual tagging of samples to detect any cross-over during PCR, 5) Dual indexing of libraries to detect any tag jumps, 6) Matching to manually cross-checked reference library.

4. The full animal *sed*aDNA record

The full animal *sed*aDNA record includes 85 animal taxa detected in 244 of samples and is provided in Supplementary Fig. 4.1. Note that for the overview Fig.1 in the main text, the two sequences identified to *Anser* are merged, although their separate occurrences in samples suggest that they may represent different species. Note also that according to the CONISS analyses, the major division in the animal community is at 4.1 ka cal BP with further zone divisions at 12.4 and 0.55 ka cal BP.

We note that some species that are found in the region today, were not detected in *sed*aDNA. For Grey wolf, the sequence sharing with dogs challenge reliable identification (Supplementary Table S2), as dog DNA may also come from reagents (see above). Other regional species include arctic fox (*Vulpes lagopus*), Eurasian lynx (*Lynx lynx*), common shrew (*Sorex araneus*), Eurasian otter (*Lutra lutra*) and the mustelids least weasel (*Mustela nivalis*) and stoat (*Mustela erminea*). In the warmer parts of the Holocene, roe deer (*Capreolus capreolus*) would also be possible. As these taxa are all represented in the DNA reference library, the lack of detection is not due to the lack of a reference. Bones of Eurasian otter are recorded in the region (Supplementary Table S4) and the lack of *sed*aDNA could for most sites be explained by the distance to the sea. Mountain hare and European water vole were detected earlier in bones than in *sed*aDNA, and the earliest records of reindeer and hare were surprisingly late compared to its early arrival in western Norway [36]. The other species are also lacking from the regional bone records (Supplementary Table S4). For example, lynx are also rare in archaeological records, and their past distribution is therefore largely unknown [37]. Overall, we detected mammals in 58% of the sample with on average 0.94±1.15 species per sample (63% of samples last 6 k with 1.25±1.26 species). This is similar to what has been found overall for a circumpolar study of 495 samples (1.86 taxa, 63% of samples), and higher than found in lake sediments (38% of samples with 0.69 taxa, [32], suggesting that our methods worked well. Thus, the low carnivore detection may be related to low biomass abundance, leaving only scattered *sed*aDNA that is challenging to detect.

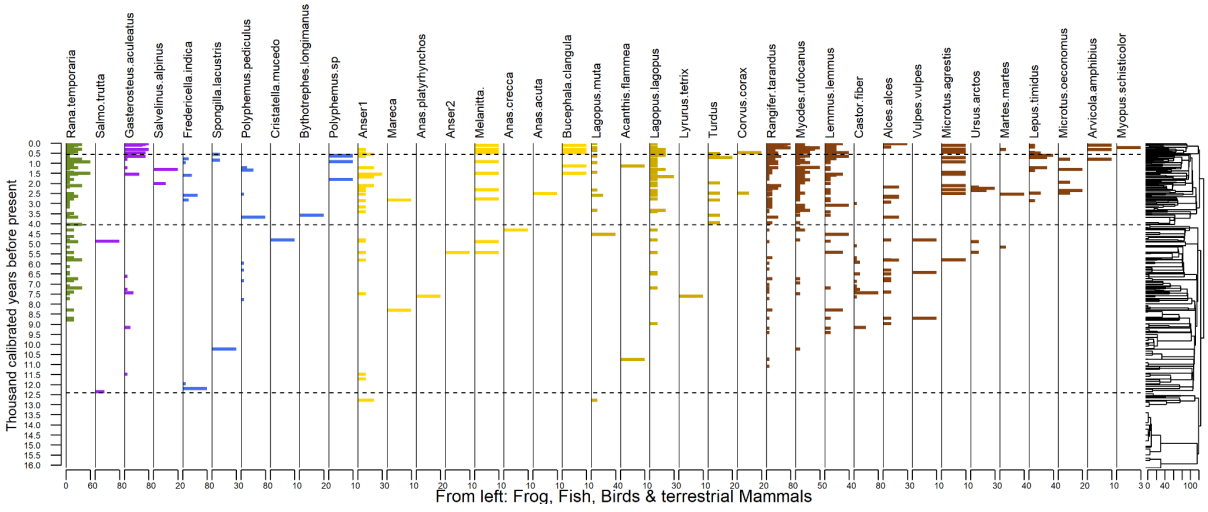

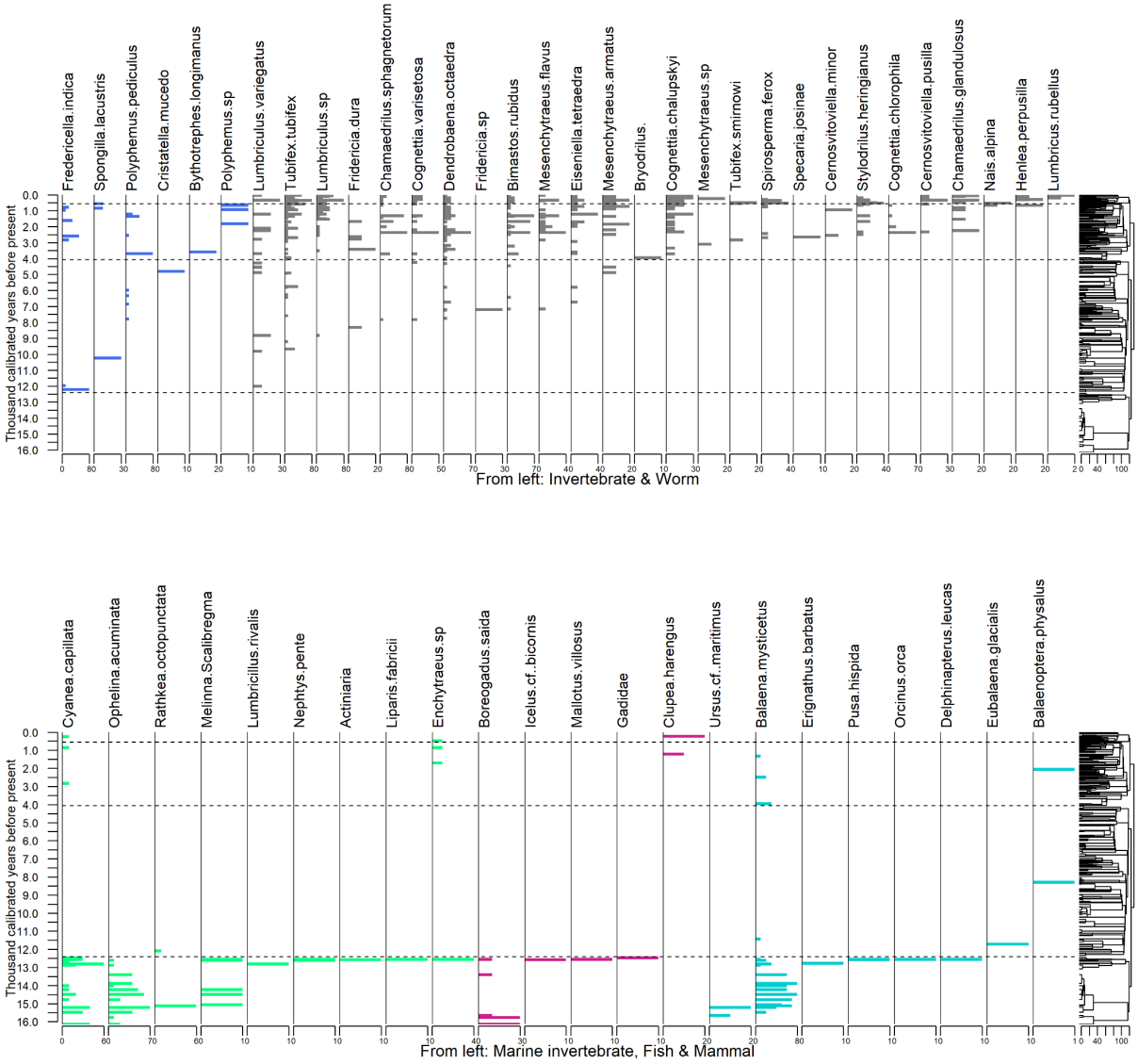

Supplementary Fig. 4.1 Identification of animals in ten sediment cores from N Fennoscandia. The quantification is given as numbers of PCR repeats (1-8); note the difference in scale between taxa. ***a*** *Terrestrial and freshwater vertebrates (green=amphibian, purple=fish, yellow=bird, brown=mammals).* ***b****, Freshwater invertebrates (blue) including worms (grey, mostly assumed to be freshwater/terrestrial).* ***c****, Marine organisms (green=invertebrate, purple=fish, and blue=mammal).*

5. Comparison of bone and *sed*aDNA records

Of the 12 mammal taxa identified, all were recorded in *sed*aDNA and eight were recorded as bones. Note that quantification is uncertain based on both methods, but the bone records were clearly strongly biased towards reindeer (Supplementary Fig. 5.1), which, based on the bone record, is assumed to have been a major part of the human diet in the region [38].

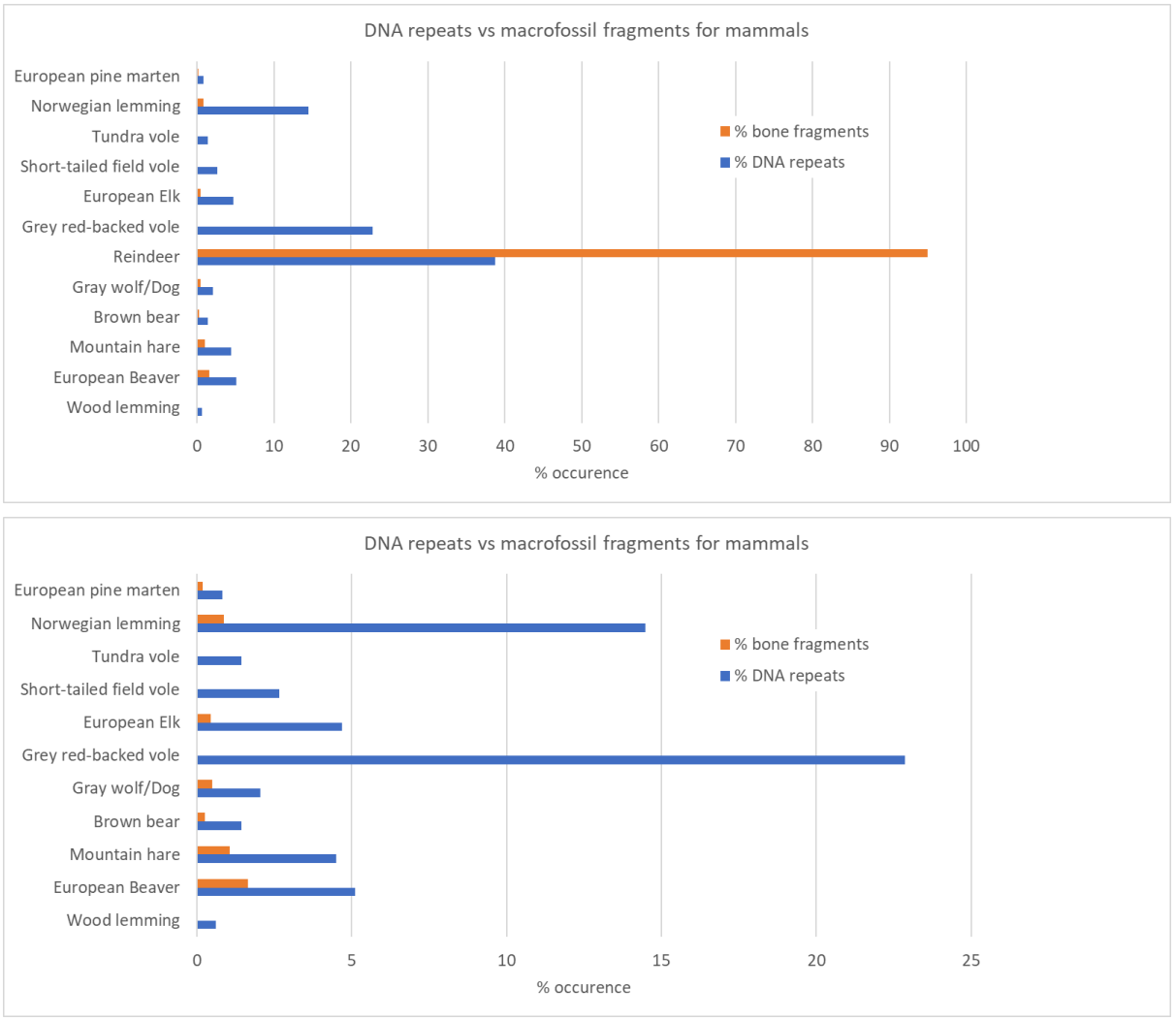

Supplementary Fig. 5.1 Relative abundance of taxa detected in sedaDNA (% of repeats) and bone fragments (% of fragments). ***a****, All mammals.* ***b****, Excluding reindeer.*

6. Animal frequency over time

Both numbers of samples and numbers of animals detected increased towards the present (Supplementary Fig. 6.1a-b). However, the proportion of samples that contained the total record of mammals, or the individual species (reindeer, Norwegian lemming, grey-sided vole, willow ptarmigan and frog) also increased towards the present (Supplementary Fig. 6.1c-h), showing that the increase is not only due to sampling effort. Moreover, as the *sed*aDNA quality was stable over this time period [22], we assume that the increase in detection represents a true increase in occurrences, as also seen by the increase in sites where reindeer was detected (Supplementary Fig. 6.2).

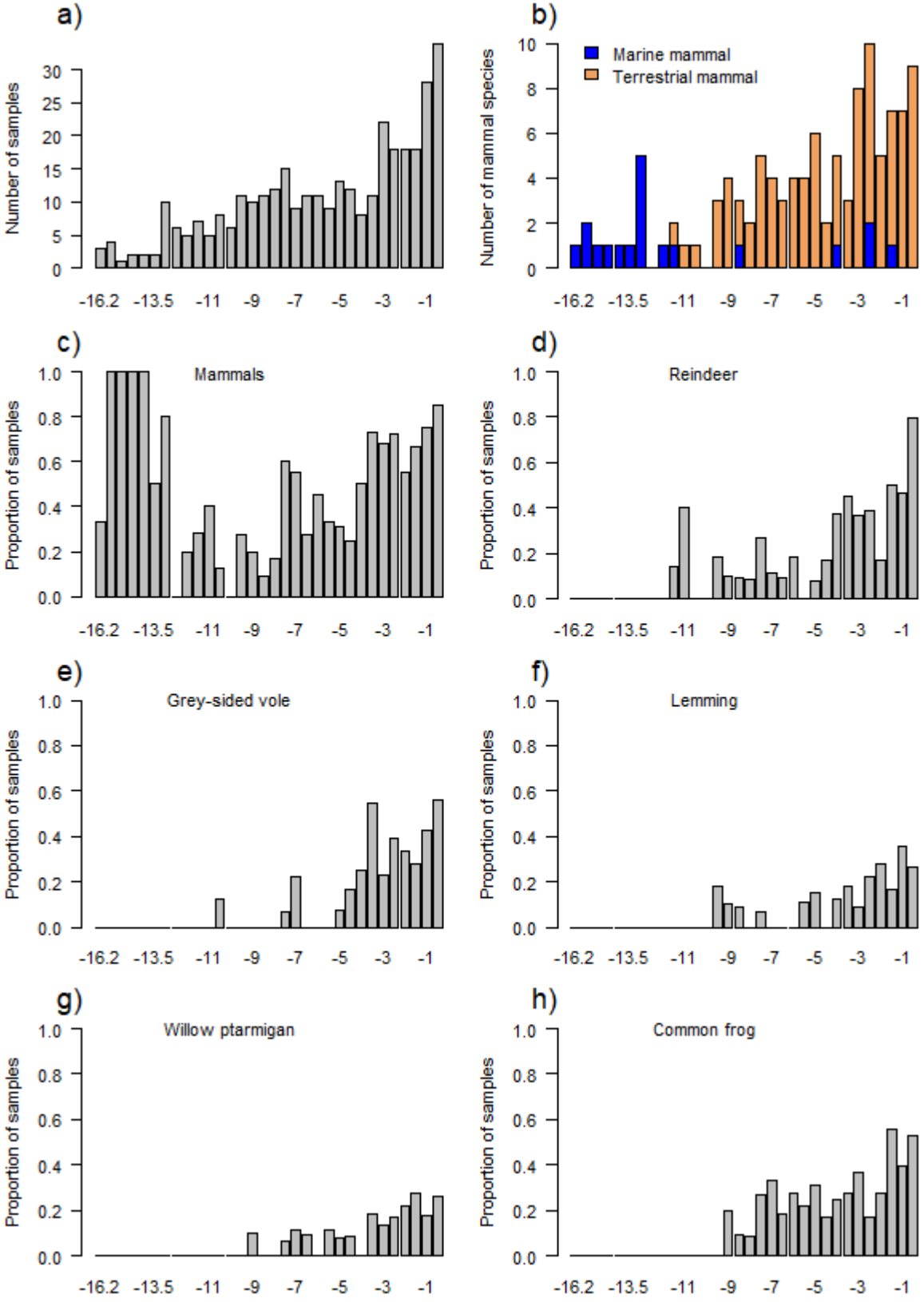

Supplementary Fig. 6.1 Density of sampling and detection of animals in sedaDNA analysis per 500 year time interval. ***a****, Number of samples.* ***b****, Number of mammals species detected. Proportion of samples with* ***c****, total mammals,* ***d****, reindeer,* ***e****, grey-sided voles,* ***f****, lemmings,* ***g,*** *willow ptarmigan, and* ***h,*** *frog.*

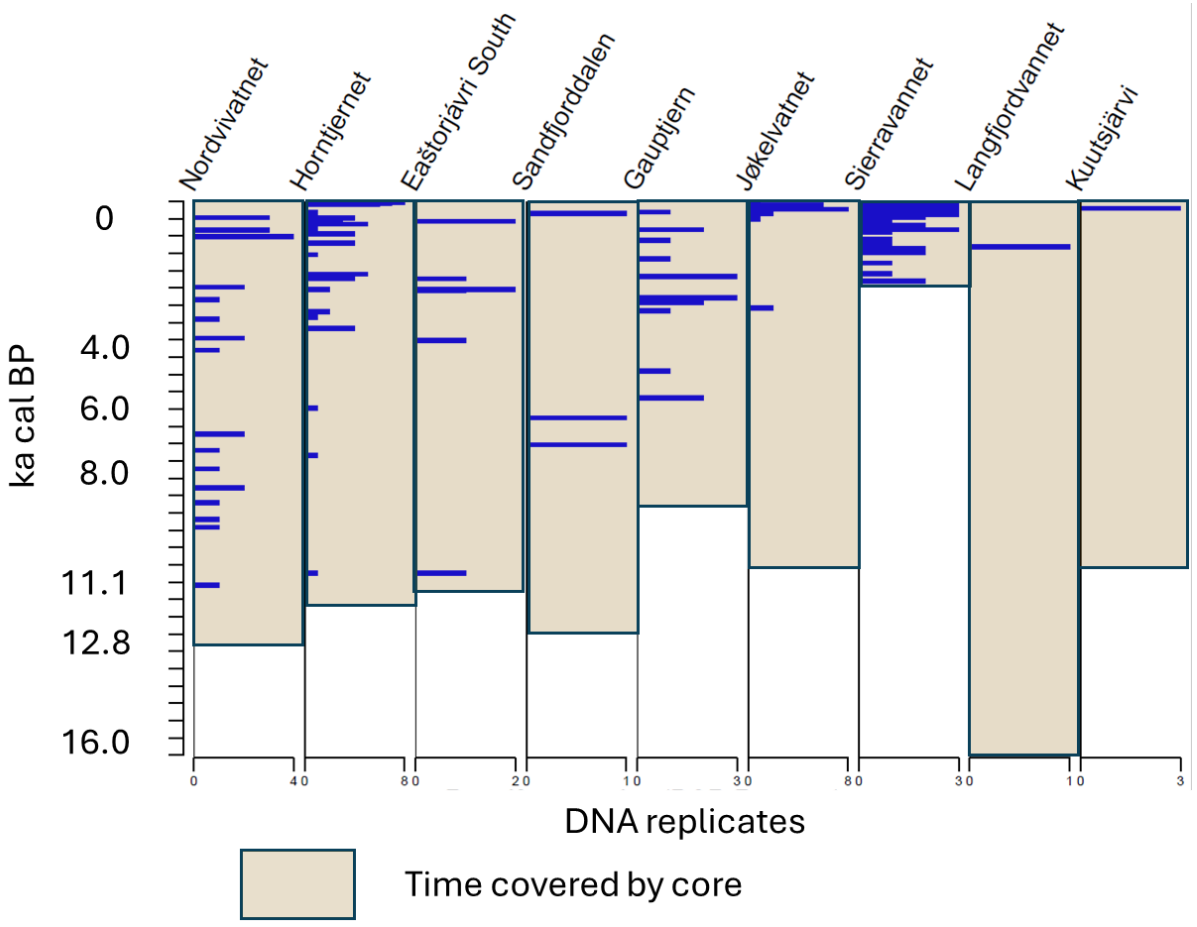

Supplementary Fig. 6.2. Reindeer appearance at the nine sites it was recorded (there were no records of reindeer from Nesservatnet on the island Årøya). Lake Jøkelvatnet is on a peninsula where dispersal is limited by a glacier and steep hillsides, Langfjordvannet is on the northern island of Arnøya, and lake Kuutsjävri is presently dominated by spruce and pine forest.

7. Plant-herbivore co-occurrence networks

We plotted co-occurrence networks for significant co-occurrences across three methods only (Fig. 2), and for 75% co-occurrences (Supplementary Fig. 7.1). We show all 1474 co-occurrence in Supplementary Table 6 along with the plant traits and significant levels according to our different tests. We are not aware of any similar data even for the present that shows plants-herbivores co-occurrence, but the patterns fit with the habitat description of individual species as for example described in the Norwegian encyclopaedia Store Norske Leksikon (https://snl.no/“).

7.1 Reindeer co-occurrence

Reindeer showed both significant and >75% co-occurrence with *Empetrum nigrum, Rubus/Fragaria* (presumably *Rubus chamaemorus*), *Juniperus communis* and *Pinus sylvestris.* These plant taxa appeared before reindeer, although *Pinus sylvestris* did not appear regularly until 10.3 ka cal BP and *V. myrtillus* appeared 10.5 ka cal BP (Supplementary Table S6, [28]). Most of these taxa are known as common food plants to reindeer [39,40]. Reindeer further showed >75% co-occurrence the common food plants *Vaccinium myrtillus, V. uliginosum, V. vitis-idaea, Betula, and Salicaceae.*. The plants co-occurring with reindeer have generally wide habitats, but there is a high proportion of graminoids and woody species mainly growing in sub-alpine or forest.

7.2 Grey-sided vole co-occurrence

There were 21 plant taxa with >75% co-occurrence with grey-sided vole, 12 of them significant. This included tall forbs such as *Angelica archangelica, Trollius europaeus,* and *Filipendula ulmaria* as well as several ferns and trees and small forbs. All except threeof these were present prior to first detection of grey-sided vole. There were 37 additional plant taxa showing significant co-occurrence with grey-sided vole, 22 of them arriving after the first appearance of grey-sided vole. Important food plants as *Empetrum nigrum, Vaccinium uliginosum, V. myrtillus,* and *V. vitis-idaea* were identified as significant in two of the three approaches whereas *Betula* and *Salicaceae* were co-occurring in almost all samples but not significantly. The 75% co-occurring plant taxa represent all growth forms and a wide range of habitats from arctic-alpine like *Oxyria digyna* and *Harrimanella hypnoides* to boreal like *Pinus sylvestris, Linnea borealis* and *Matteuccia struthiopteris.*

7.3 Norwegian lemming co-occurrence

There were 14plant taxa that showed 75% or more co-occurrence with Norwegian lemming, but only one of them significantly accordign to all three test (*Gymnocarpium*). Other taxa with 75% co-occurrence inluded *Vaccinium uliginosum, Empetrum nigrum, Betula, Gymnocarpium,* Carduinae*, Juniperus communis, Rubus/Fragaria* (presumabley *Rubus chamaemorus*), *Solidago virgaurea* and *Saussurea/Lactuca.* The former four are also found in Norwegian lemming diet [41,42]. There were a further five plant taxa with >75% co-occurrence of which Salicaceae, *Vaccinium myrtillus, V. vitis-idaea* and *Bistorta vivipara* are known food items [41,42] and *Sorbus aucuparia* a likely food item. A further 26 plant taxa

showed significant co-occurrence according to all three test. These include food plants like *Rumex* and several graminoids, and overall a large species typical for low to high alpine sites like *Silene acaulis, Diapensia lapponica* and *Orojuncus trifidus.*

7.4 Willow ptarmigan

There were 19 plant taxa that showed 75% or more co-occurence with willow ptarmigan, This included many species with berries: *Sorbus aucuparia, Juniperus communis, Vacconium vitis-idaea, V. myrtillus, V. uliginosum, Empetrum nigrum* and *Rubus/Fragaria* (presumabley *Rubus chamaemorus*). Further, tall (*Angelica archangelica, Filipendula ulmaria*) and small (*Bistorta vivipara, Solidago cf virgaurea, Saussurea alpina*) and a small fern (*Gymnocarpium*), as well as the alway precent *Betula* and *Salicaceae*. The *Vaccinium* species and *Empetrum* are also found in eDNA analyses of diet in the region, whereas *Bistorta* is an important food item in general for ptarmigan [43,44]. A further 17 taxa showed significant co-occurrence according to all three tests (Supplementary Table S6). T. Of the 22 plant taxa that showed significant co-occurrence, 9 arrived after willow ptarmigan.

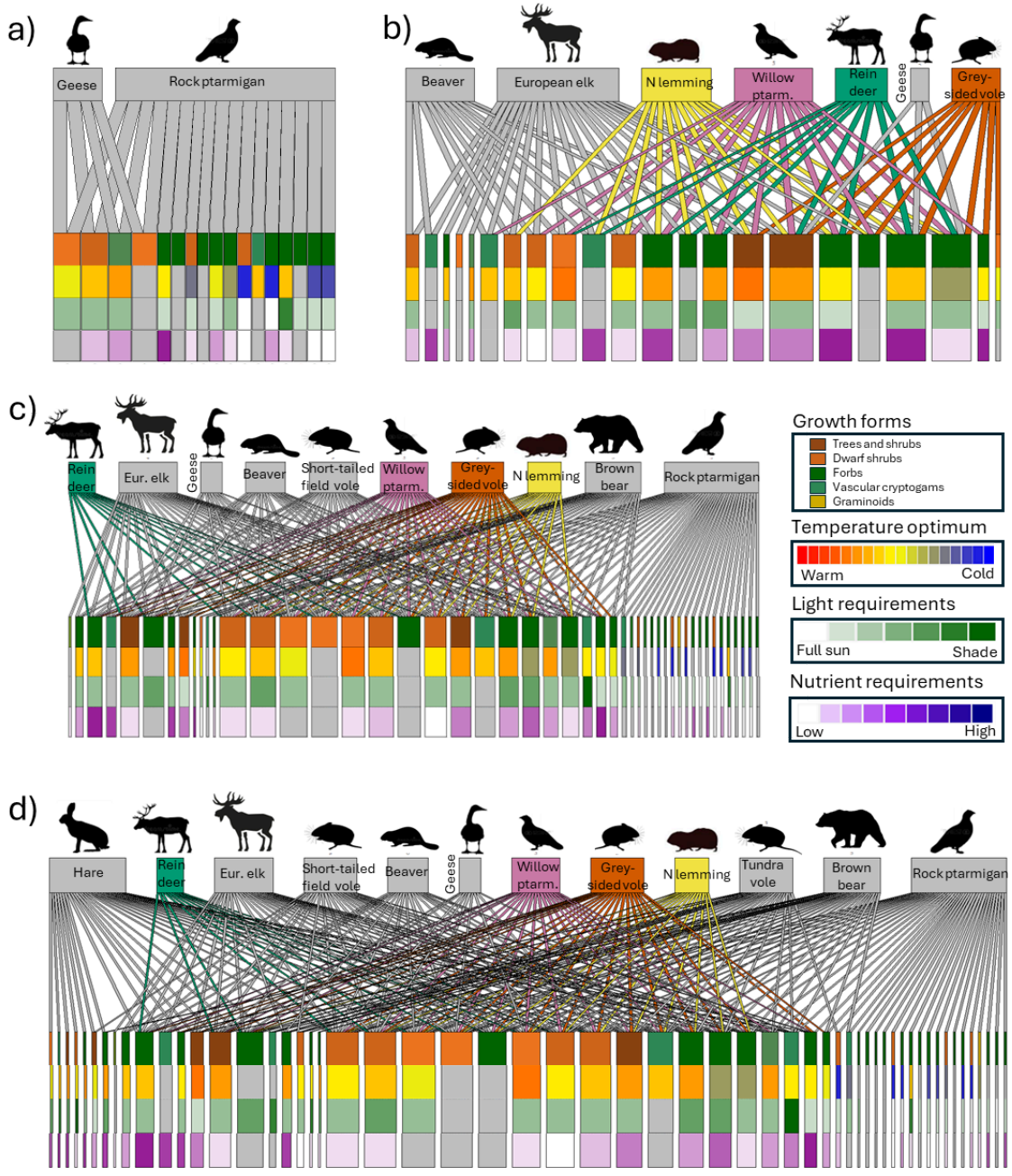

Supplementary Fig. 7.1. Herbivore network for 75% co-occurrence. ***a****, Late Glacial (12.8-11.7 ka BP).* ***b****, Early Holocene (11.1-8.3 ka BP).* ***c****, Middle Holocene (8.2-4.259* ***d****, Late Holocene* (≥4.25 ka cal BP). *Animal symbols as in Fig. 1. The omnivore brown bear is here plotted as a herbivore.*

7.5 Strength of plant-herbivore associations

To further explore whether there were consistent differences in the vegetation in samples were herbivores were present or not detected, we tested for differences in plant species richness (number of terrestrial vascular plants detected) between samples with and without reindeer or small rodents, as well as differences in the relative abundance (proportion of reads) of forbs and graminoids in the vegetation. Both forbs and graminoids are preferred food items of herbivores and plant groups that have been shown to benefit from herbivory.Reindeer were marginally associated with plant communities with higher richness and occurred with slightly higher abundance of graminoids (richness: 1.199; Standard error SE = 0.100; 95% confidence interval CI = -0.015 - 0.379; z = 1.807; p = 0.071. Proportion of reads: 0.027, SE = 0.013, 95% CI = 0.001 - 0.053; z = 2.070, p = 0.039; Supplementary Fig. 6.5a), whereas the six small rodents taken together were associated with plant communities with higher vascular plant richness, especially forb richness (valscular plant richness: 0.089; SE = 0.028; 95%CI = 0.033 - 0.144; < = 3.14, p = 0.002. Forb richness: 0.115; SE = 0.042; 95%CI = 0.032 - 0.197; < = 2.732; p = 0.006) Supplementary Fig. 6.5b). The difference in mean species richness values was low, suggesting that the interaction between plants and herbivores was not a very important driver of plant richness patterns (Fig. 1a). This finding is in strong contrast to the Alps, where a strong increase in species richness, especially the forb component of plant communities, was reported in response to the introduction of domesticated mammals [45]. Northern Fennoscandia is the region with the greatest number of studies on Arctic contemporary herbivores, and the majority of those show low impact of herbivores on plant community compositions, likely because the winter conditions keep herbivores at low densities [46]. Thus, our findings of past plant-herbivore associations confirm the general findings based on contemporary studies.

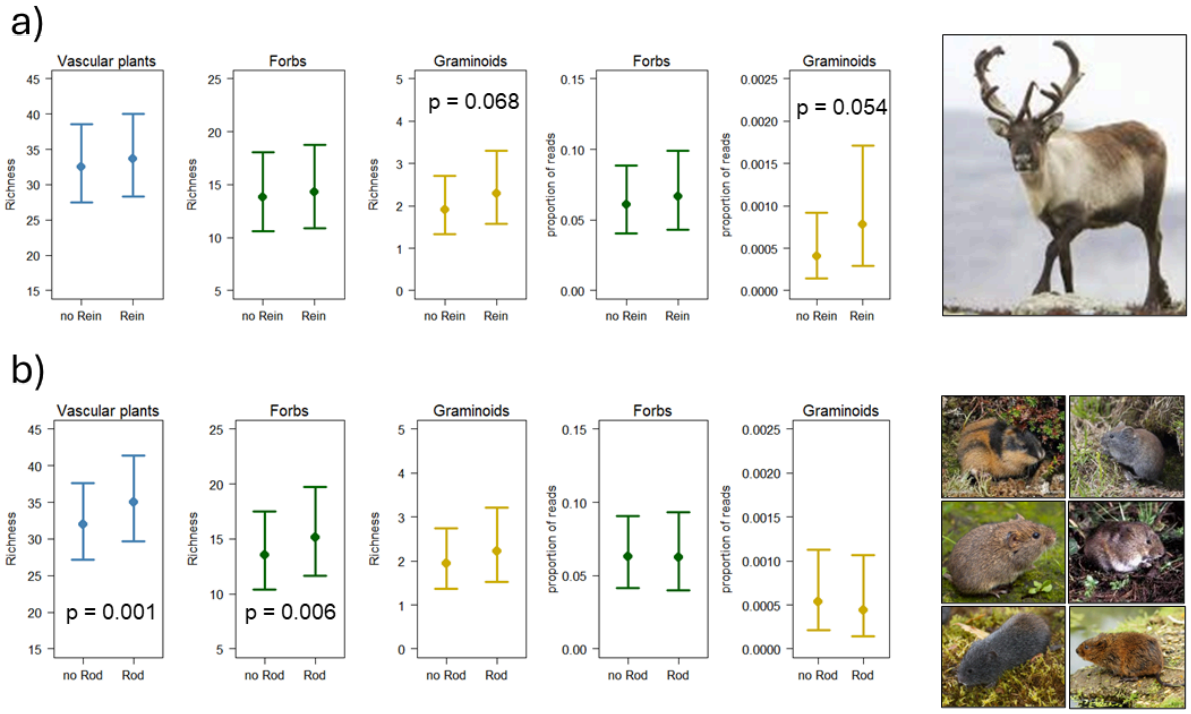

Supplementary Fig. 7.5 Relationships between herbivore presence and plant abundance and richness for selected plant growth forms (forbs and graminoids). ***a,*** *Impact of reindeer*

(Rein; Rangifer tarandus*), and* ***b,*** *impact of all small rodents (Rod) found in the region. From the top left: Norwegian lemming (*Lemmus lemmus*), grey-sided vole (*Myodes rufocanus*), short-tailed field vole (*Microtus agrestis*), tundra vole (*Microtus oeconomus*), wood lemming (*Myopus schisticolor*) and European water vole (*Arvicola amphibius*).*

8. Niche change for individual species

8.1 Changes in niche sizes

Both niche size (Supplementary Fig. 8.1) and niche dimensions (Supplementary Figs. 8.2-8.6) changed over time. Below, we provide some comments on the individual species, whereas the overall pattern is displayed and described in the main text.

a)

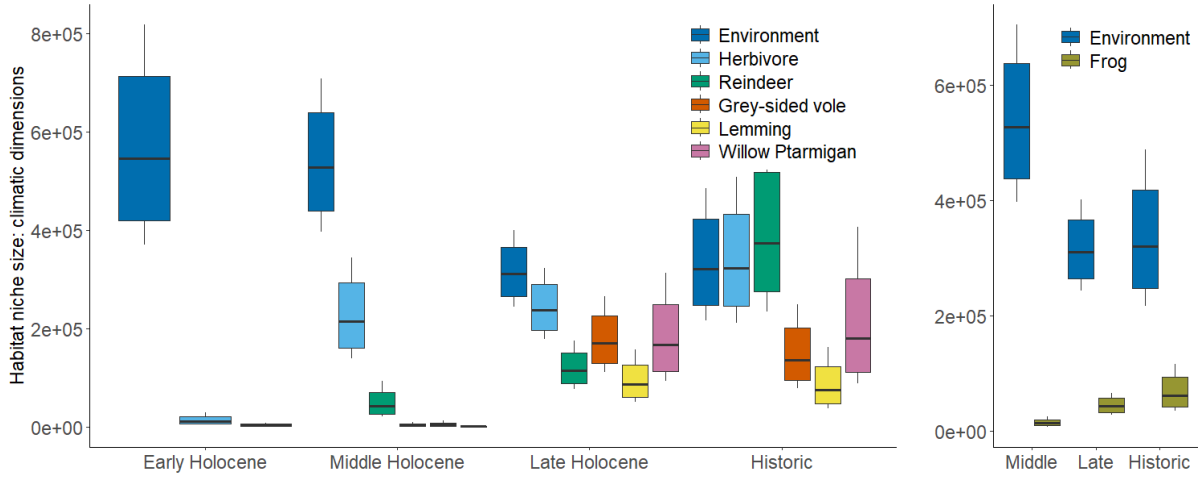

b)

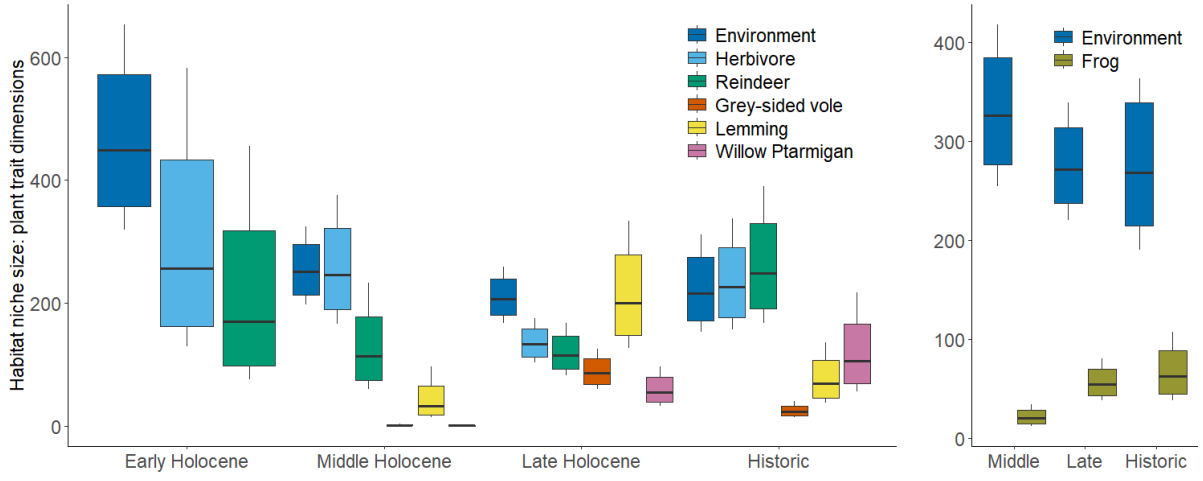

c)

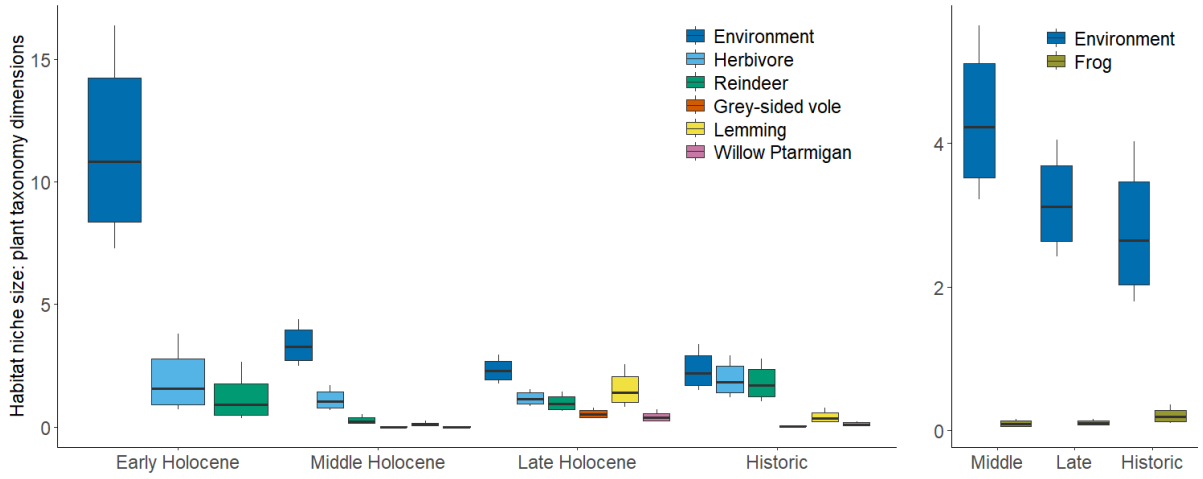

d)

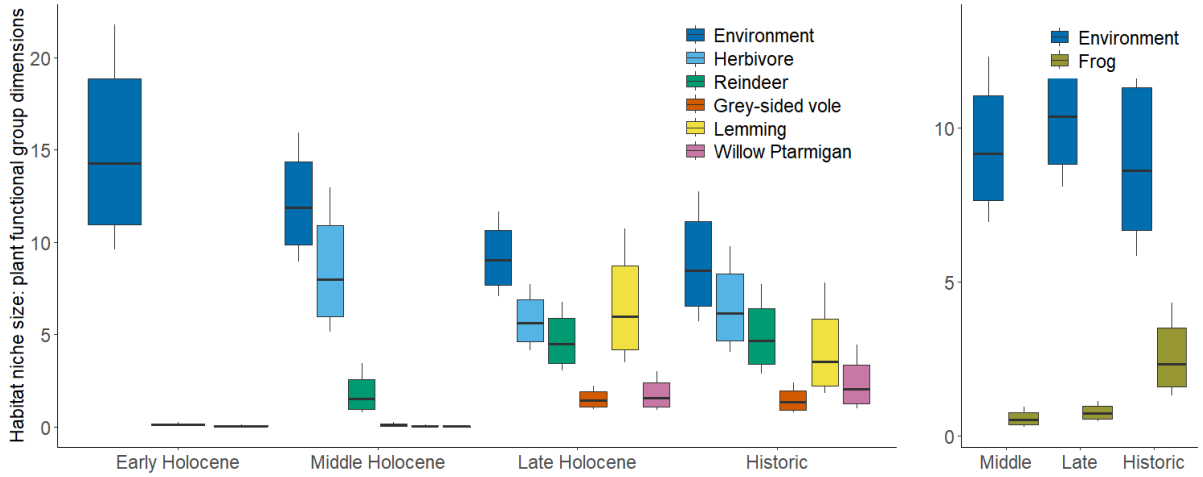

Supplementary Fig. 8.1. Niche size for different niche dimensions and time periods for each of five species. ***a,*** *Climatic niche,* ***b,*** *abiotic plant traits,* ***c,*** *plant taxonomic diversity,* ***e,*** *plant functional groups.*

8.2 Reindeer niche

The single niche dimension that predicted reindeer occurrence best was annual precipitation, followed by taxonomic diversity NMDS dimension1, July temperature and functional diversity NMDS dimension 4 (Fig.3a). The set of niche dimensions that explained the occurrence of reindeer best was climate (44%) followed by plant taxonomic diversity (26%), whereas plant abiotic traits and plant functional groups explained 14-15%. Reindeer mainly occurred in samples with annual precipitation below 550 mm and July temperature of 10-15°C.

There were large changes in niche dimensions, especially the climate niche, with less than 20% probability of overlap among 8 of the 12 comparisons among time periods (Supplementary Fig. 8.2a). There was less shift in abiotic traits based on plants, with about 90% probability of the niche from Late Holocene being found within the present day niche

(Supplementary Fig. 8.2b). Similarly, the largest shifts in plant taxonomic diversity and plant functional traits were from Early to Middle and Middle to Late Holocene, with a smaller shift from Late Holocene to the Historical time period (Supplementary Fig. 8.2c, d). When all 15 niche dimensions were analysed together, the largest change in niche was between the two most recent periods compared to the two oldest periods (Supplementary Fig. 8.2e).

The size of the climatic and abiotic niche are significantly increasing in the last 650 years, probably because humans brought the reindeer to new sites where they do not occur naturally. This is further confirmed by their occupation of almost all environmental space for climate, abiotic traits and plant taxonomic diversity, whereas their niche sizes in earlier periods only occupy a fraction of the environmental spaces (Fig. 3).

Reindeer have large ranges and show annual migration between different habitats. Their diet is broad, with a high number of vascular plants, bryophytes and lichens identified [40,47], and their most common food items are widespread in the region. In contrast, their heat tolerance is low [48] and the accessibility of food may be limited by snow and ice during winter [49]. This might explain why climate niche dimensions seem more important than vegetation for reindeer.

a)

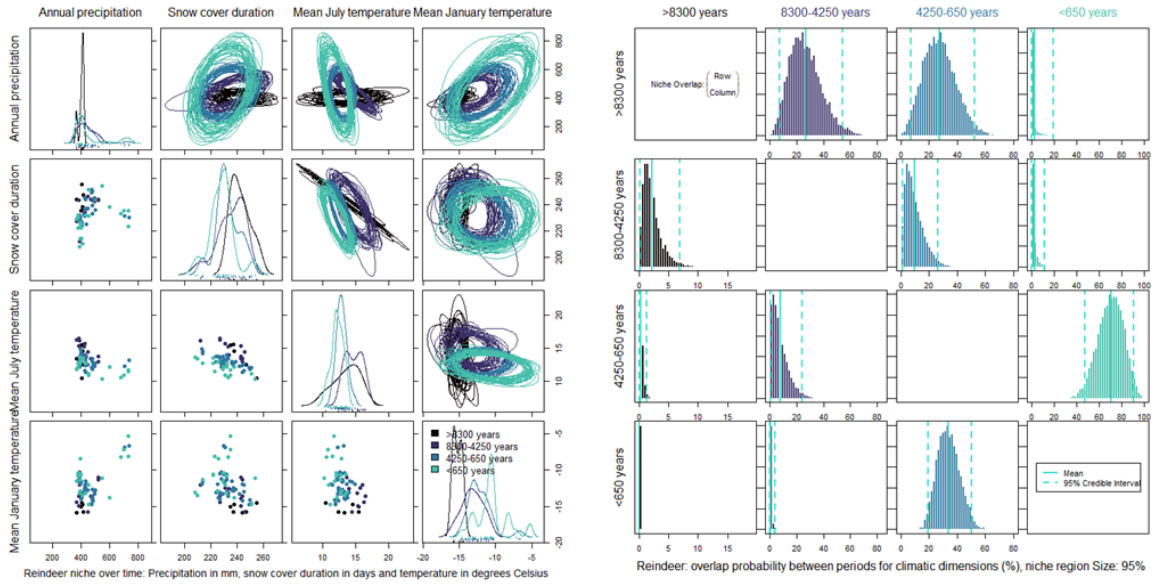
Annual precipitation
Snow cover duration
Mean July temperature
Mean January temperature
>8300 years
8300-4250 years
4250-650 years
<650 years
Niche Overlap
Row
Column
Mean
95% Credible Interval
Reindeer niche over time: Precipitation in mm, snow cover duration in days and temperature in degrees Celsius
Reindeer: overlap probability between periods for climatic dimensions (%), niche region Size: 95%

b)

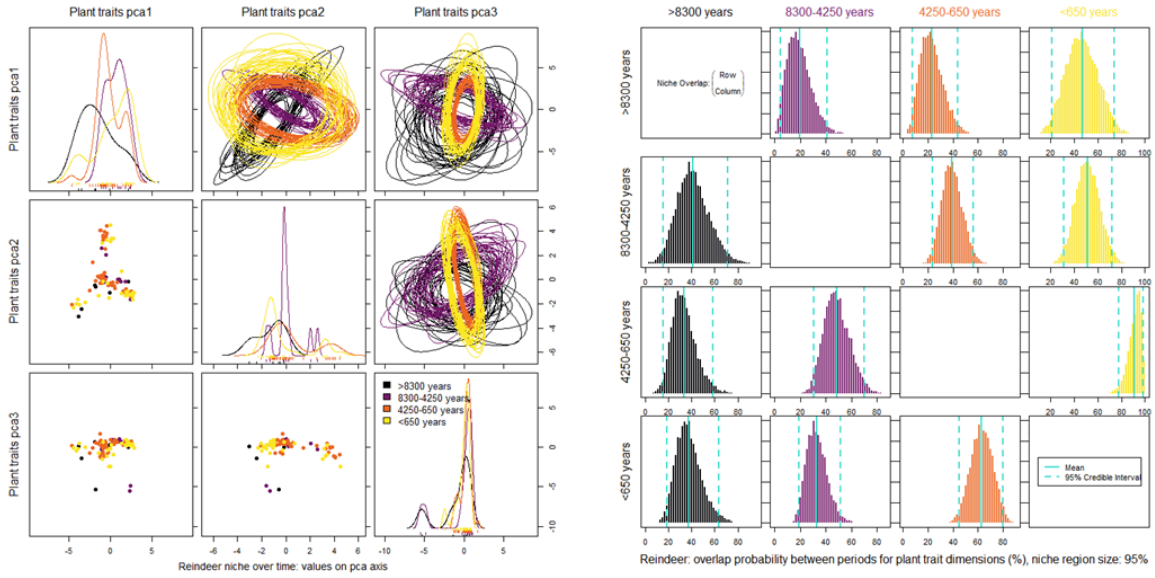
Plant traits pca1
Plant traits pca2
Plant traits pca3
>8300 years
8300-4250 years
4250-650 years
<650 years
Niche Overlap
Row
Column
Mean
95% Credible Interval
Reindeer niche over time: values on pca axis
Reindeer: overlap probability between periods for plant trait dimensions (%), niche region size: 95%

c)

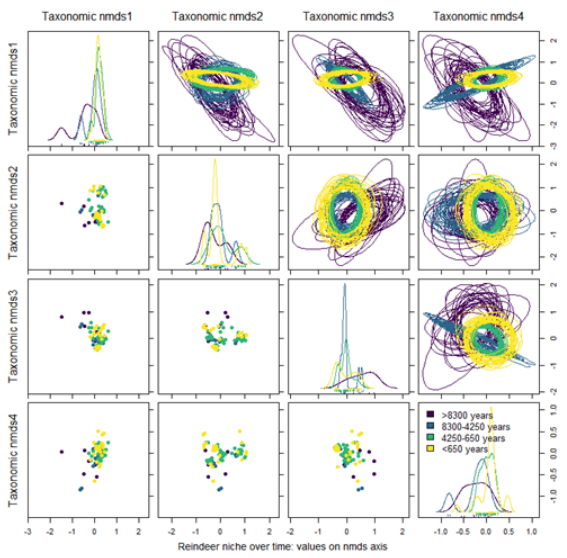
Taxonomic nmds1
Taxonomic nmds2
Taxonomic nmds3
Taxonomic nmds4
>8300 years
8300-4250 years
4250-650 years
<650 years
Reindeer niche over time: values on nmds axis

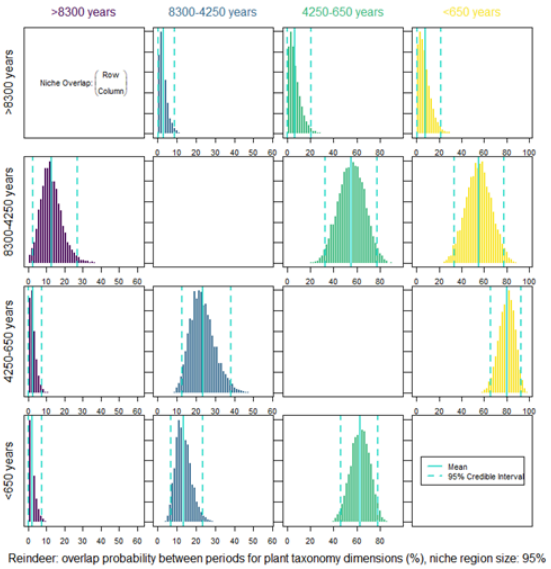
>8300 years
8300-4250 years
4250-650 years
<650 years
Niche Overlap:
Row
Column
Mean
95% Credible Interval
Reindeer: overlap probability between periods for plant taxonomy dimensions (%), niche region size: 95%

d)

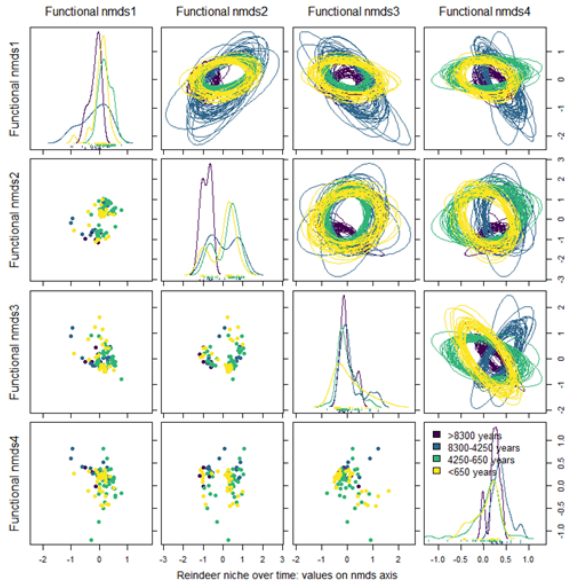
Functional nmds1
Functional nmds2
Functional nmds3
Functional nmds4
>8300 years
8300-4250 years
4250-650 years
<650 years
Reindeer niche over time: values on nmds axis

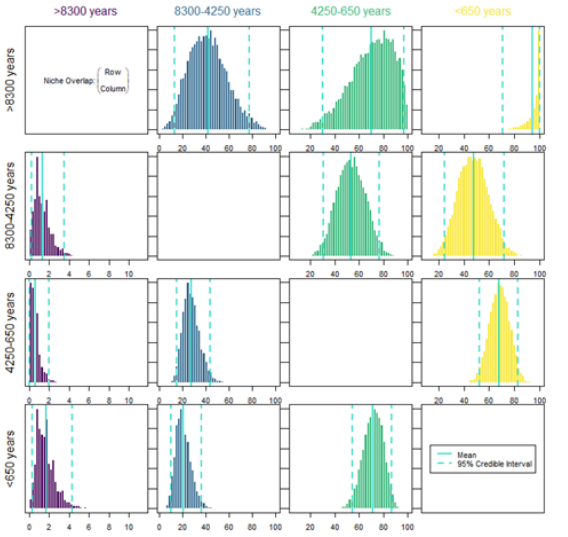
>8300 years
8300-4250 years
4250-650 years
<650 years
Niche Overlap:
Row
Column
Mean
95% Credible Interval
Reindeer: overlap probability between periods for plant functional group dimensions (%), niche region size: 95%

e)

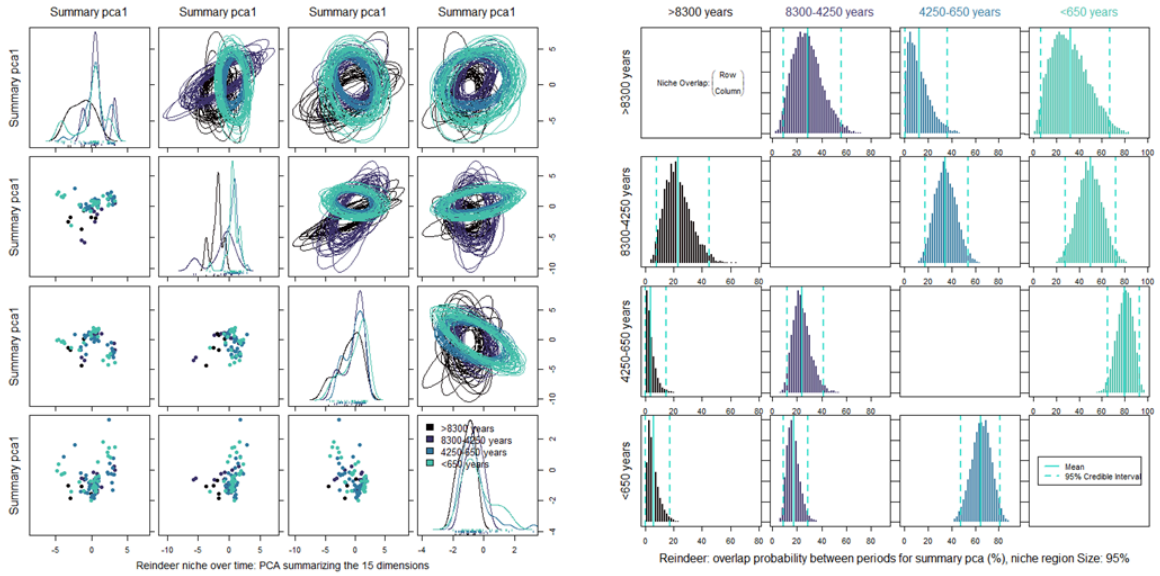

Supplementary Fig. 8.2. Niche stability over time for ***reindeer*** *(*Rangifer tarandus*) based on* ***a****, climate niche dimension,* ***b,*** *climate and other abiotic conditions inferred from the traits of plants present,* ***c,*** *vegetation attributes with emphasis on taxonomic richness,* ***d,*** *vegetation attributes using with emphasis on abundance of plant functional composition,* ***e,*** *all 15 niche dimensions summarised using 3 PCA axis representing 70% of the variation. The bar plots represent the posterior probability that an individual from the time period indicated by the row will be found within the niche of the time period indicated by the column header.*

8.3 Grey-sided vole niche

Grey-sided vole occurrence was best predicted by taxonomic diversity NMDS dimension 1 followed by abiotic traits dimension2 and taxonomic diversity NMDS dimension 2. The niche that best explained its occurrence was taxonomic dimensions (48%), followed by plant abiotic traits (24%), plant functional groups (15%) and climate (13%) (Fig. 3).

There were large changes in all niche dimensions over time. The probability of finding the niche of Late Holocene or Historical period in the Middle Holocene was close to zero whereas there was less change in climate niche between Late Holocene and the Historical period (Supplementary Fig. 8.3a). A very similar pattern was seen for abiotic plant traits, plant taxonomic diversity and plant functional groups (Supplementary Fig. 8.3b-d) and all 15 niche dimensions combined (Supplementary Fig. 8.3e). The probability to find the Historical niche dimensions in Late Holocene was medium for climate (~50%), and high for the other sets of niches and the combination of all 15 niche dimensions (60-85%).

The size of the plant abiotic traits and plant taxonomic diversity niche was largest in Late Holocene and decreased the last 650 years (Supplementary Fig. 8.1). This is surprising, given that the proportion of samples with grey-sided voles increased towards the present, but we do note that the frequency was also high around 4000 years ago (Supplementary Fig. 6.1e). The climatic niche showed minor change over the same period, suggesting that the

reduction is related to biotic interactions. A reduction could potentially be caused by human mediated range expansion and population increase of reindeer, as these species show increased overlap over time (see below). This contradicts contemporary co-occurrence studies based on faeces counts that suggest that reindeer may facilitate small rodents [50], although rodents were not distinguished to species, and therefore it is uncertain if this applies to grey-sided vole. The increase in niche overlap may not exclude other causes for niche size reduction in grey-sided vole, for example increased predation or competition from other rodents.

a)

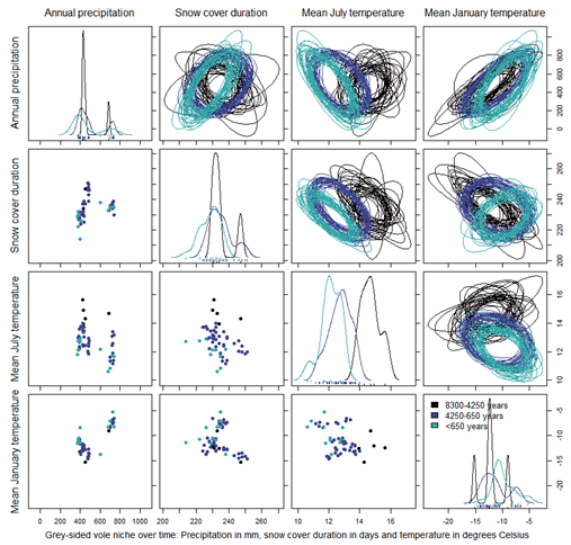
Annual precipitation
Snow cover duration
Mean July temperature
Mean January temperature
8300-4250 years
4250-650 years
<650 years
Grey-sided vole niche over time: Precipitation in mm, snow cover duration in days and temperature in degrees Celsius

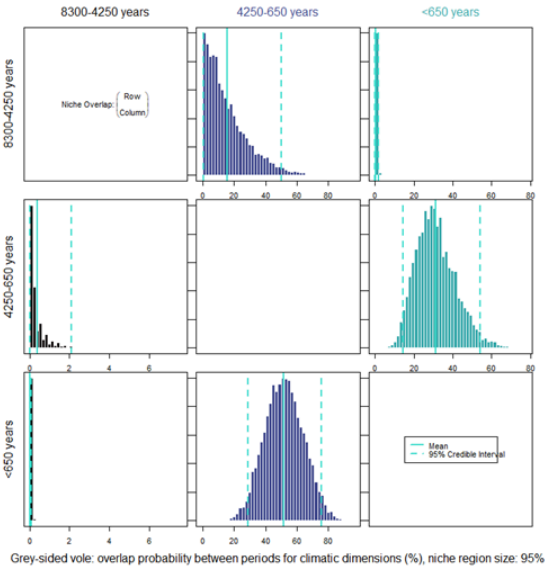
8300-4250 years
4250-650 years
<650 years
Niche Overlap:
Row
Column
Mean
95% Credible Interval
Grey-sided vole: overlap probability between periods for climatic dimensions (%), niche region size: 95%

b)

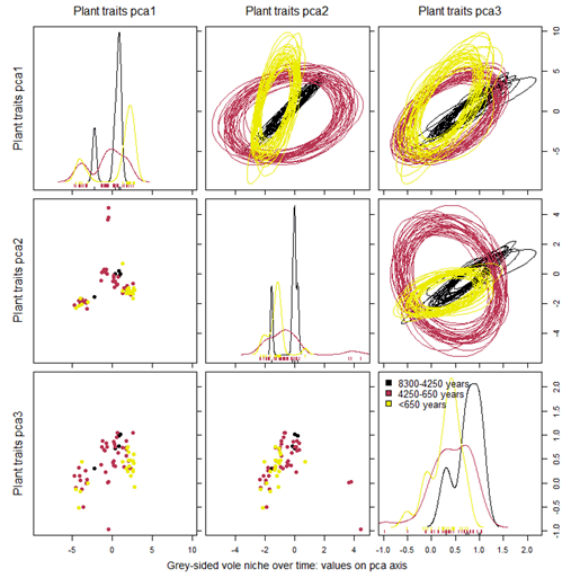
Plant traits pca1
Plant traits pca2
Plant traits pca3
8300-4250 years
4250-650 years
<650 years
Grey-sided vole niche over time: values on pca axis

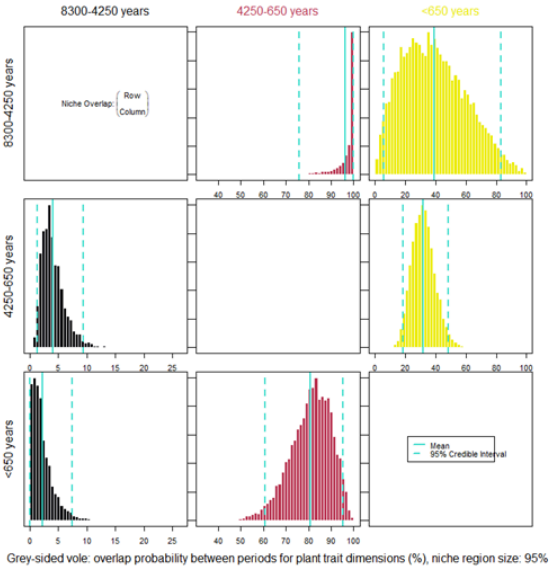
8300-4250 years
4250-650 years
<650 years
Niche Overlap:
Row
Column
Mean
95% Credible Interval
Grey-sided vole: overlap probability between periods for plant trait dimensions (%), niche region size: 95%

c)

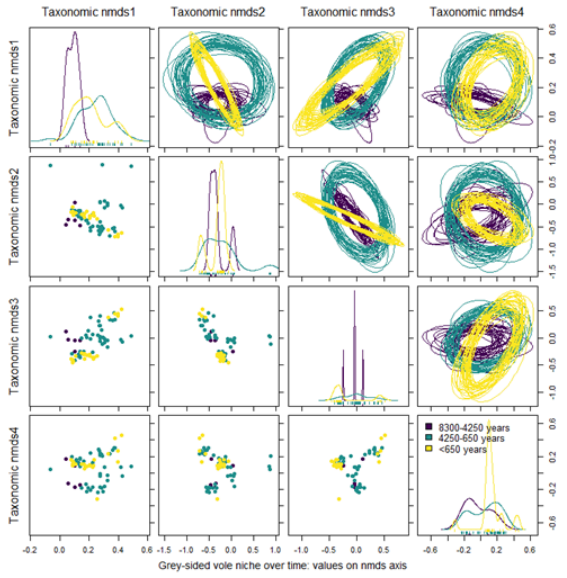

Grey-sided vole niche over time: values on nmds axis

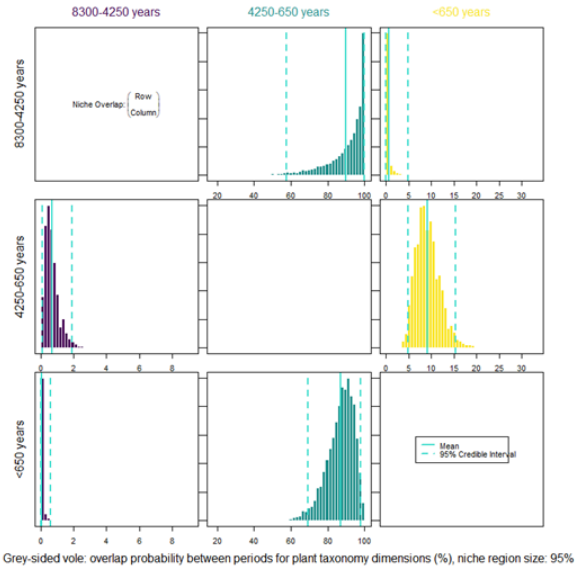

Grey-sided vole: overlap probability between periods for plant taxonomy dimensions (%), niche region size: 95%

d)

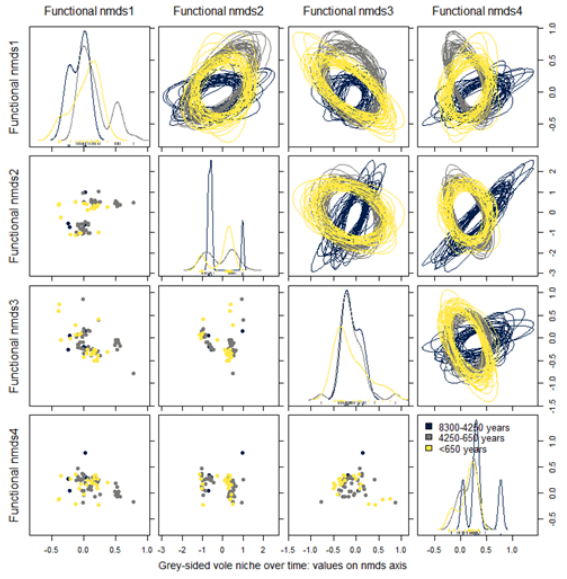

Grey-sided vole niche over time: values on nmds axis

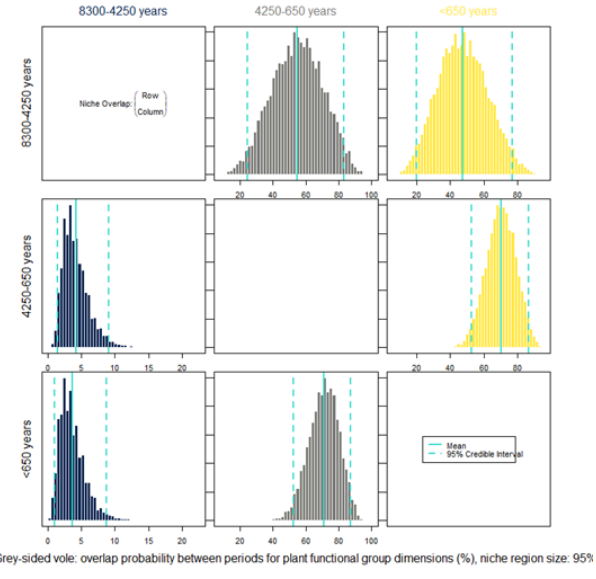

Grey-sided vole: overlap probability between periods for plant functional group dimensions (%), niche region size: 95%

e)

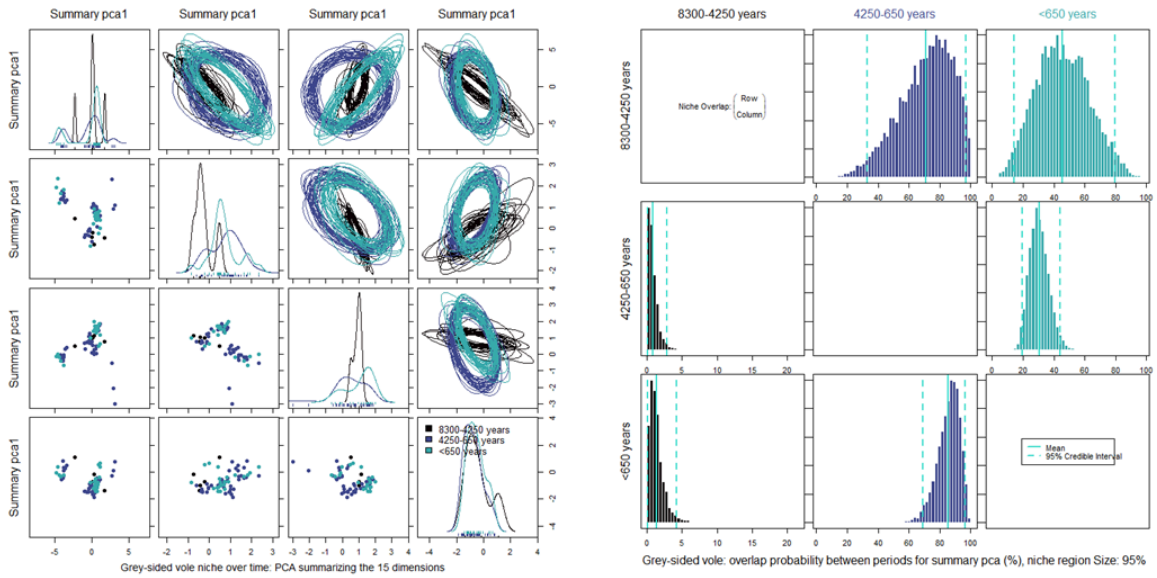

*Supplementary Fig. 8.3. Niche stability over time for **grey-sided vole** (*Myodes rufocanus*) based on **a**, climate niche dimension, **b,** climate and other abiotic conditions inferred from the traits of plants present, **c,** vegetation attributes with emphasis on taxonomic richness, **d,** vegetation attributes using with emphasis on abundance of plant functional composition, **e,** all 15 niche dimensions summarised using 3 PCA axis representing 70% of the variation. The bar plots represent the posterior probability that an individual from the time period indicated by the row will be found within the niche of the time period indicated by the column header.*

8.4 Norwegian lemming niche

The occurrence of Norwegian lemming was best predicted by plant taxonomic richness NMDS dimension 2, followed by annual precipitation, plant taxonomic diversity NMDS dimension 1 and snow cover. Overall, the occurrence of Norwegian lemming was marginally better predicted by plant taxonomic diversity (37%) than climatic niche dimensions (33%), whereas plant functional groups and abiotic traits predicted 19% and 11%, respectively (Fig. 3).

The pattern of change in climate niche dimension of Norwegian lemming is surprisingly similar to that of grey red-sided vole: the probability of finding the niche of Late Holocene or Historical period in the Middle Holocene was close to zero whereas there was less change in climate niche between Late Holocene and the Historical period (Supplementary Fig. 8.4a). The change in abiotic plant traits was similar to that of climate (Supplementary Fig. 8.4b), and also to that of grey red-sided vole (Supplementary Fig. 8.3b). Similarly, there was close to zero probability of finding the plant functional niche of the Middle Holocene in later periods, whereas the overlap was somewhat higher for plant abiotic traits and plant taxonomic diversity (Supplementary Fig. 8.4b-d). The probability of finding the niche from the Historical period in the Late Holocene was low for climate niches (~21%) but high for the

three others (60-80%) as well as the combination of all 15 niche dimensions (~81%, Supplementary Fig. 8.4).

The abiotic and plant taxonomic diversity niche dimensions were largest in Late Holocene and a similar trend was also seen for plant functional type niche dimensions (Supplementary Fig. 8.1). This was also the overall pattern based on all 15 individual niche dimensions (Fig. 3c). Thus, similar to grey-sided vole, the niche decreased in the last 650 years whereas the niche overlap with reindeer was high 88-94% (Supplementary Table S7).

a)

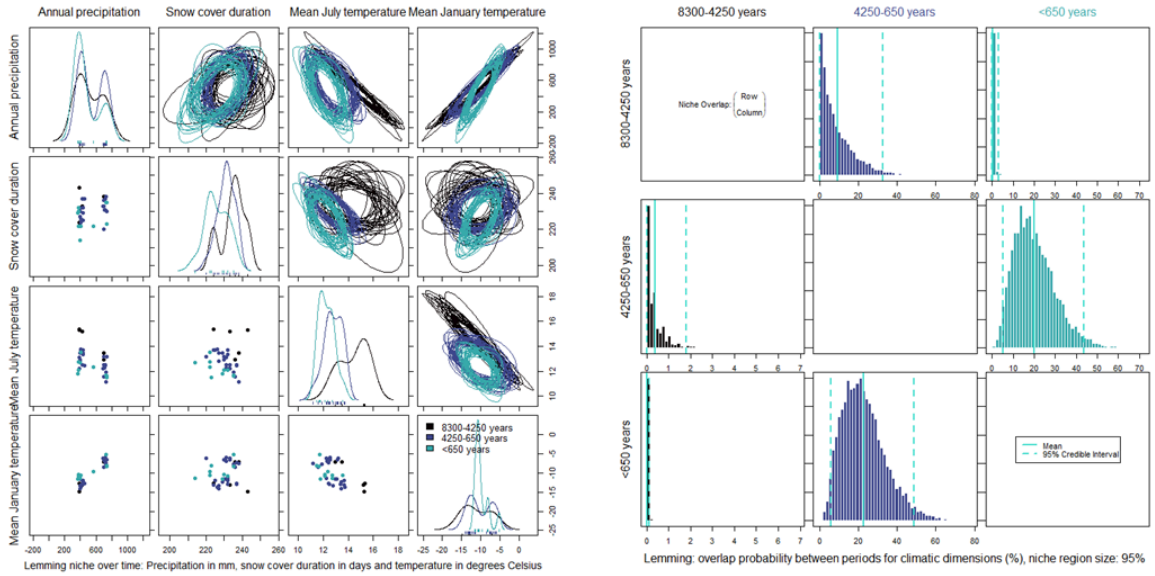
Annual precipitation
Snow cover duration
Mean July temperature
Mean January temperature
8300-4250 years
4250-650 years
<650 years
Niche Overlap:
Row
Column
Mean
95% Credible Interval
Lemming niche over time: Precipitation in mm, snow cover duration in days and temperature in degrees Celsius
Lemming: overlap probability between periods for climatic dimensions (%), niche region size: 95%

b)

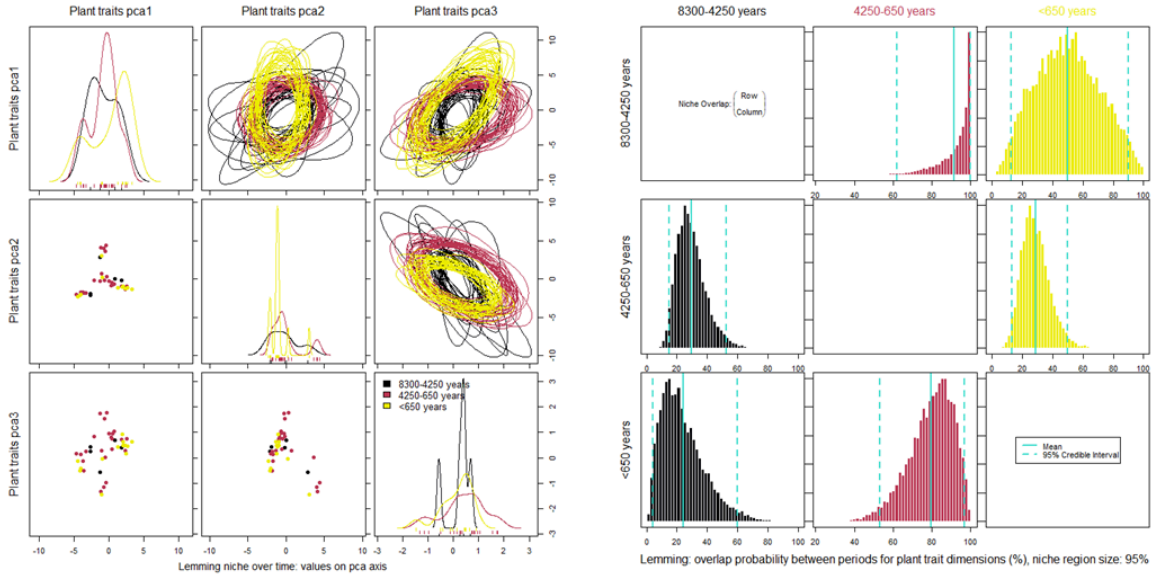
Plant traits pca1
Plant traits pca2
Plant traits pca3
8300-4250 years
4250-650 years
<650 years
Niche Overlap:
Row
Column
Mean
95% Credible Interval
Lemming niche over time: values on pca axis
Lemming: overlap probability between periods for plant trait dimensions (%), niche region size: 95%

c)

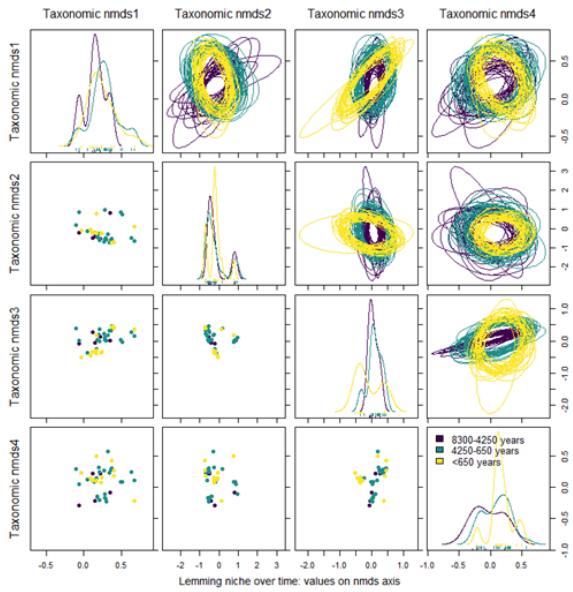
Taxonomic nmds1
Taxonomic nmds2
Taxonomic nmds3
Taxonomic nmds4
8300-4250 years
4250-650 years
<650 years
Lemming niche over time: values on nmds axis

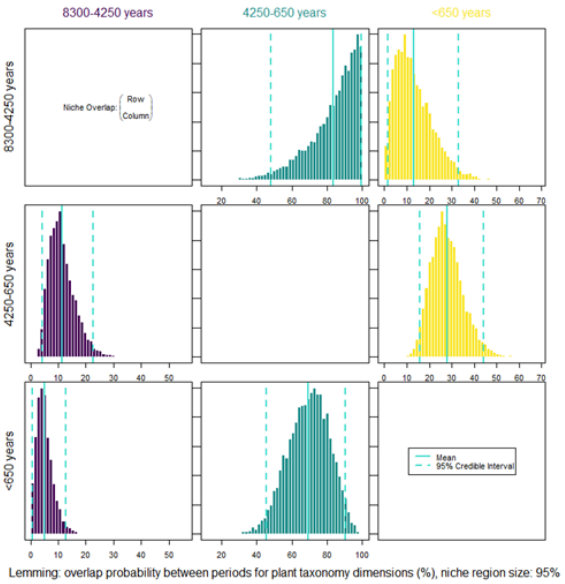
8300-4250 years
4250-650 years
<650 years
Niche Overlap:
Row
Column
Mean
95% Credible Interval
Lemming: overlap probability between periods for plant taxonomy dimensions (%), niche region size: 95%

d)

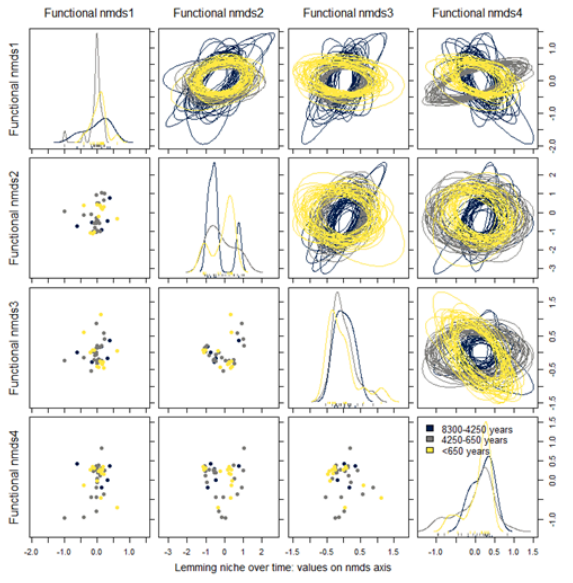
Functional nmds1
Functional nmds2
Functional nmds3
Functional nmds4
8300-4250 years
4250-650 years
<650 years
Lemming niche over time: values on nmds axis

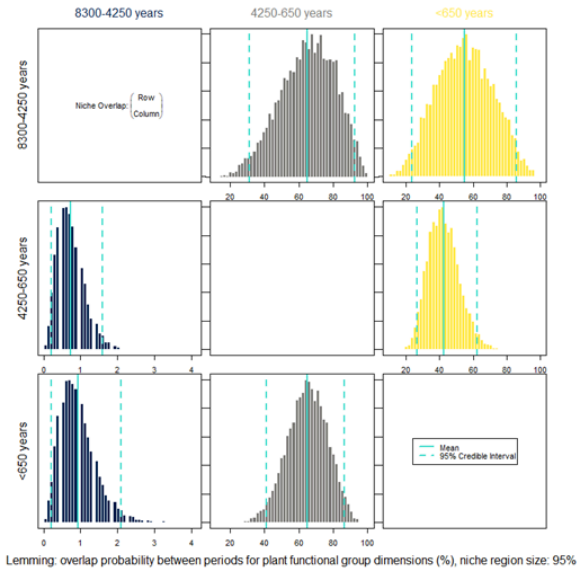
8300-4250 years
4250-650 years
<650 years
Niche Overlap:
Row
Column
Mean
95% Credible Interval
Lemming: overlap probability between periods for plant functional group dimensions (%), niche region size: 95%

e)

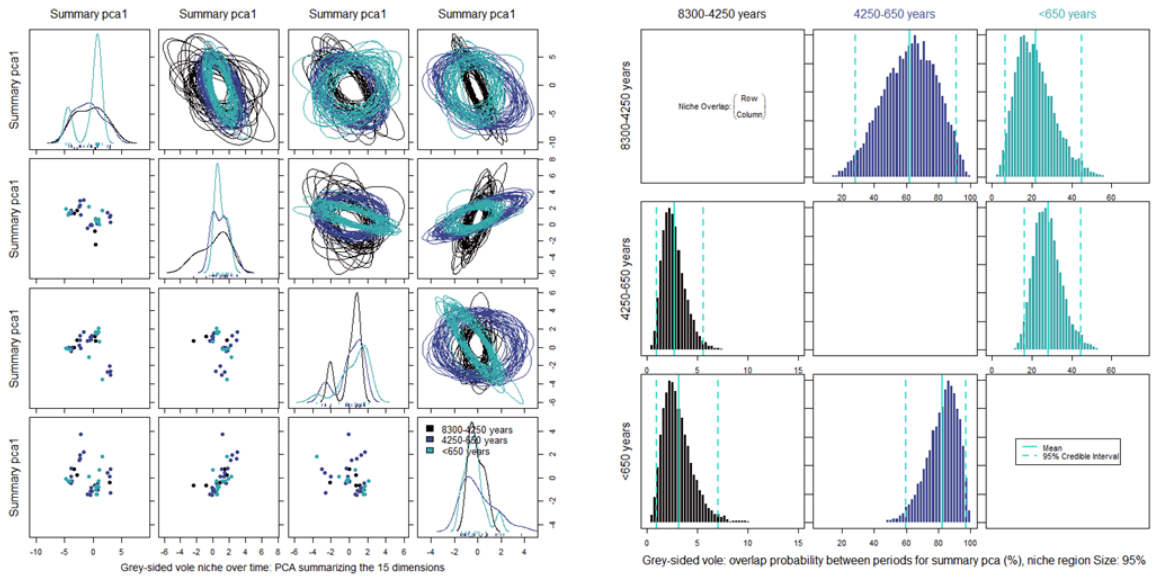

Supplementary Fig. 8.4. Niche stability over time for ***Norwegian lemming*** *(*Lemmus lemmus*) based on* ***a****, climate niche dimension,* ***b,*** *climate and other abiotic conditions inferred from the traits of plants present,* ***c,*** *vegetation attributes with emphasis on taxonomic richness,* ***d,*** *vegetation attributes using with emphasis on abundance of plant functional composition,* ***e,*** *all 15 niche dimensions summarised using 3 PCA axis representing 70% of the variation. The bar plots represent the posterior probability that an individual from the time period indicated by the row will be found within the niche of the time period indicated by the column header.*

8.5 Willow ptarmigan niche

The single niche dimension that predicted the occurrence of willow ptarmigan best was plant functional group NMDS dimension 4 followed by plant taxonomic diversity NMDS dimension 1 and abiotic traits PCA dimension 3. The set of niche dimensions that explained the occurrence of willow ptarmigan best was plant functional groups (40%) followed by plant taxonomic diversity (33%), whereas the climate (13%) and abiotic plant traits (14%) (Fig. 3).

The probability of finding the Late Holocene and Historical niche dimensions in the Middle Holocene was <5% for all four sets of niche dimensions and also for the combination of the 15 dimensions (Supplementary Fig. 8.5). For example, willow ptarmigan occurred at higher mean July temperature in the Early Holocene (12-16°C) than the Middle Holocene and Historical period (10-14°C). The probability of finding the niche dimensions of the last 650 years in Late Holocene was somewhat higher for plant taxonomic diversity (~60%) compared to climate, abiotic traits, and plant functional groups (35-50%), and was low even for all 15 dimensions combined (mean ~36%). This is also reflected in the two-dimensional niche rover plots, which show low overlap among periods.

a)

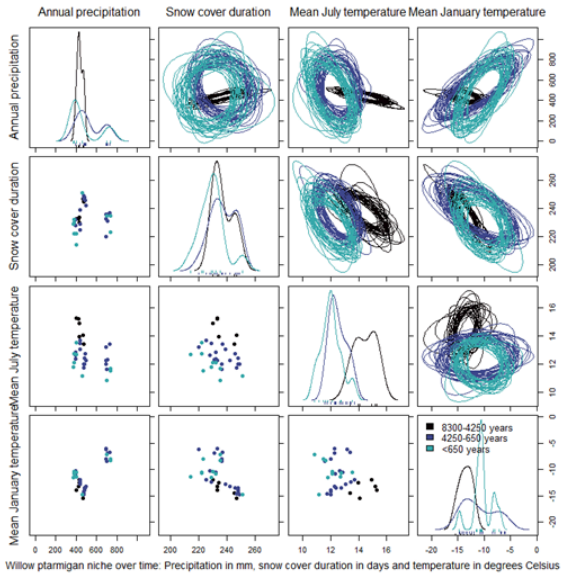

Willow ptarmigan niche over time: Precipitation in mm, snow cover duration in days and temperature in degrees Celsius

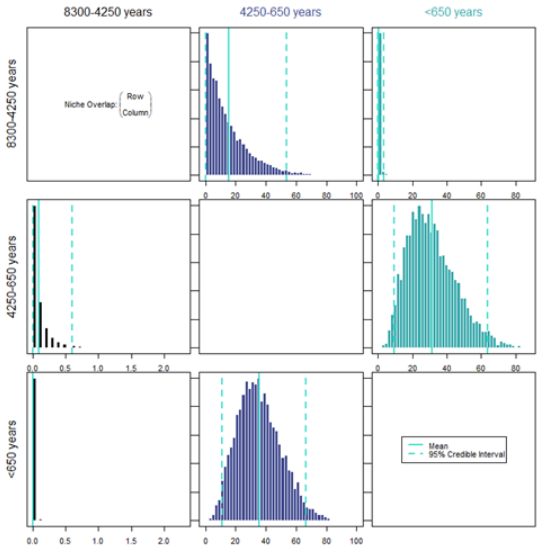

Willow ptarmigan: overlap probability between periods for climatic dimensions (%), niche region size: 95%

b)

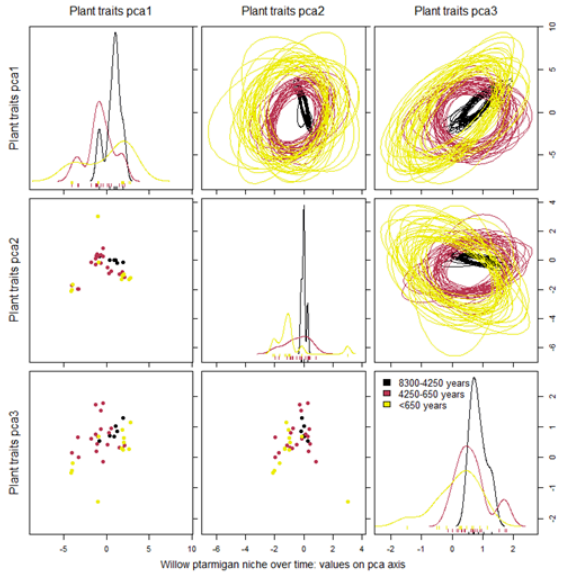

Willow ptarmigan niche over time: values on pca axis

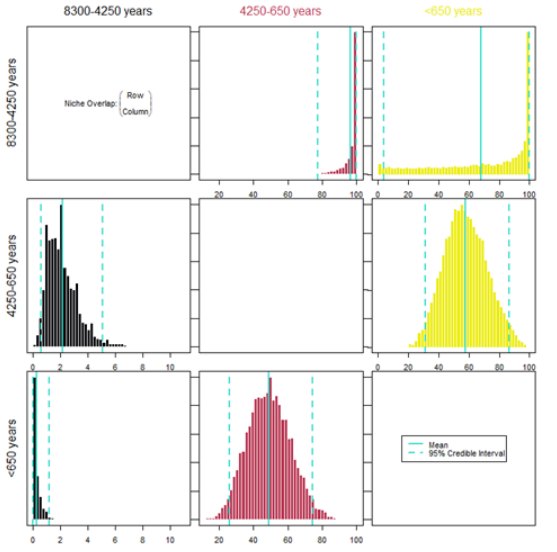

Willow ptarmigan: overlap probability between periods for plant trait dimensions (%), niche region size: 95%

642 c)

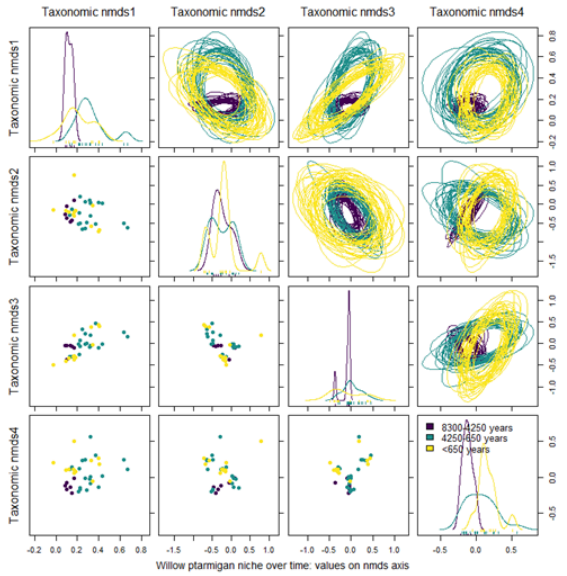

Willow ptarmigan niche over time: values on nmds axis

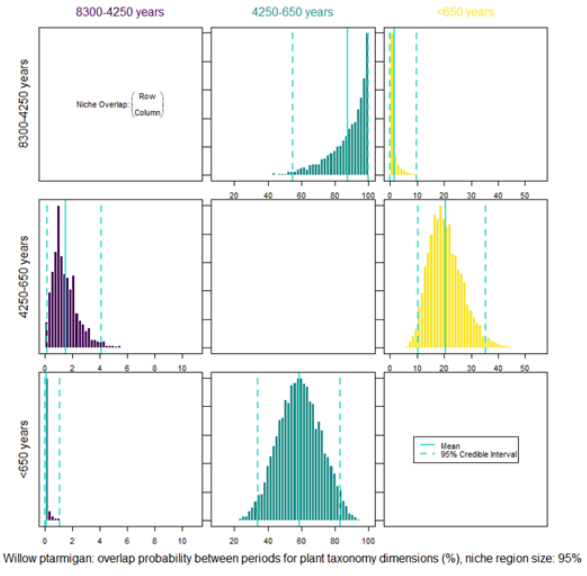

Willow ptarmigan: overlap probability between periods for plant taxonomy dimensions (%), niche region size: 95%

643

644 d)

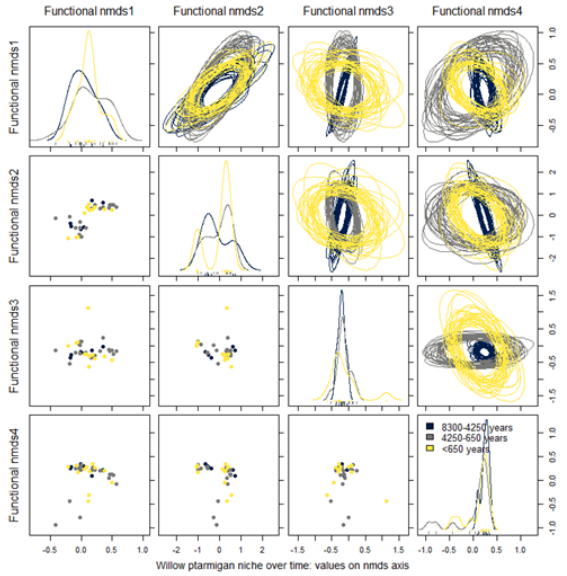

Willow ptarmigan niche over time: values on nmds axis

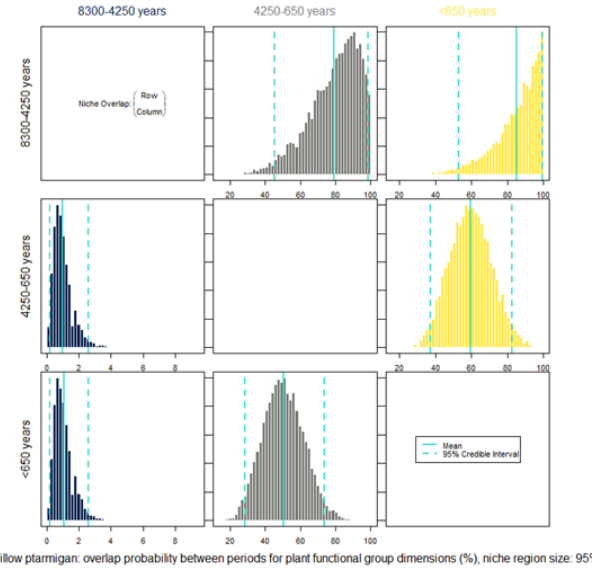

illow ptarmigan: overlap probability between periods for plant functional group dimensions (%), niche region size: 95

645

646

e)

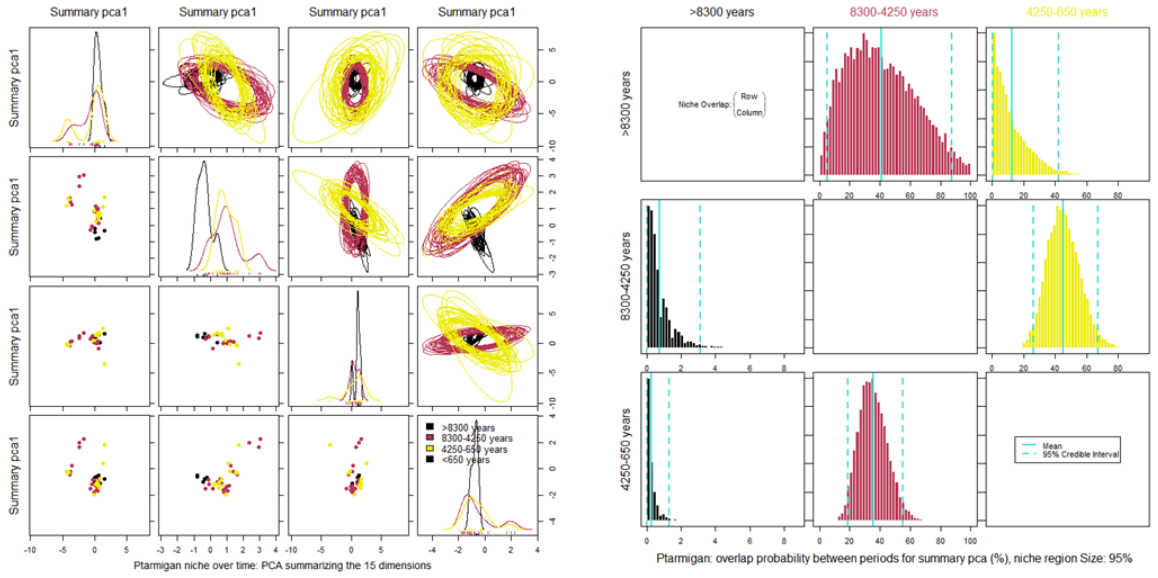

Supplementary Fig. 8.5. Niche stability over time for ***willow ptarmigan*** *(*Lagopus lagopus*) based on* ***a****, climate niche dimension,* ***b,*** *climate and other abiotic conditions inferred from the traits of plants present,* ***c,*** *vegetation attributes with emphasis on taxonomic richness,* ***d,*** *vegetation attributes using with emphasis on abundance of plant functional composition,* ***e,*** *all 15 niche dimensions summarised using 3 PCA axis representing 70% of the variation. The bar plots represent the posterior probability that an individual from the time period indicated by the row will be found within the niche of the time period indicated by the column header.*

8.6 Frog niche

Like for reindeer, the single niche dimension that predicted frog occurrence best was annual precipitation, followed by taxonomic diversity NMDS dimension1. Other important predictors were taxonomic diversity NMDS dimension 3 and plant functional groups NMDS dimension 2 (Fig. 3). Also, similar to reindeer, the set of niche dimensions that explain the occurrence of frog best was climate (39%) followed by plant taxonomic diversity (29%), whereas plant functional and plant abiotic traits explained 13% and 18%, respectively.

Except for the climatic niche (Supplementary Fig. 8.6a), there was more overlap between the Late Holocene and Middle Holocene niche for frog than for the terrestrial herbivores, with ~50% probability for abiotic plant traits, taxonomic plant diversity and plant functional groups and 40% for all 15 dimensions combined (Supplementary Fig. 8.6b-e).

As frog is both a carnivore and has exothermal regulation of body heat, it is not surprising that the climate niche dimensions predicted the occurrence best. Nevertheless, plant taxonomic diversity was the second most important niche dimension, probably reflecting characteristics of the habitat. For frog, we included the aquatic plants, and they may be good indicators of both biotic and abiotic conditions in the lake [51]. Thus, the importance of taxonomic diversity of plant may be due to aquatic plants reflecting habitat conditions adequate for the frog.

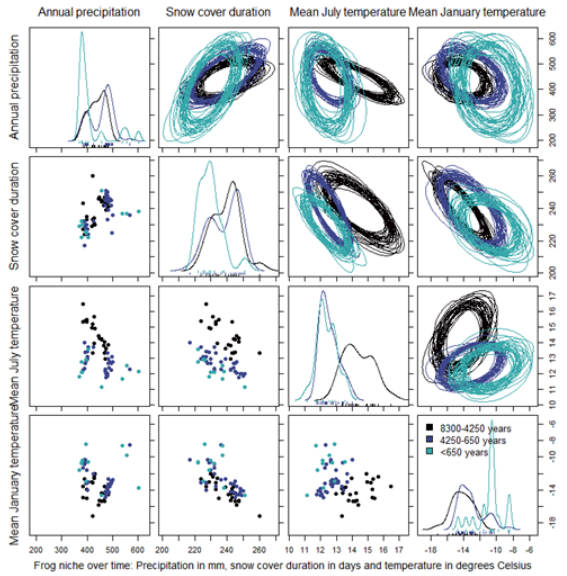

Frog niche over time: Precipitation in mm, snow cover duration in days and temperature in degrees Celsius

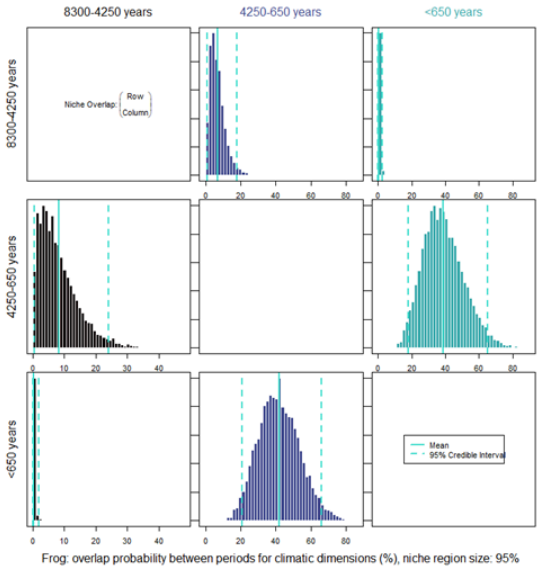

Frog: overlap probability between periods for climatic dimensions (%), niche region size: 95%

678

679

680 b)

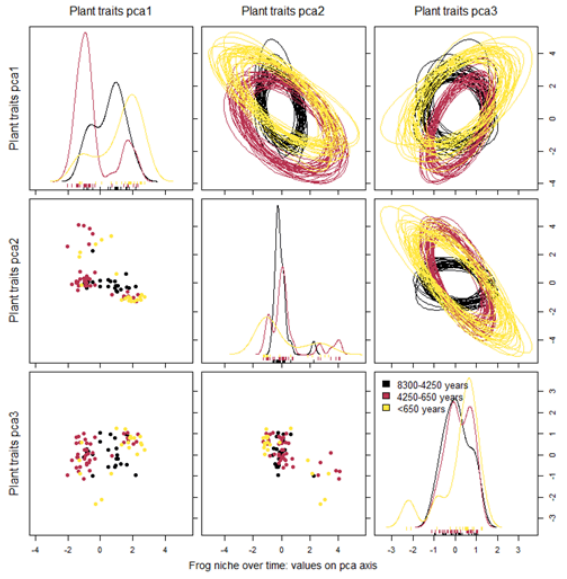

Frog niche over time: values on pca axis

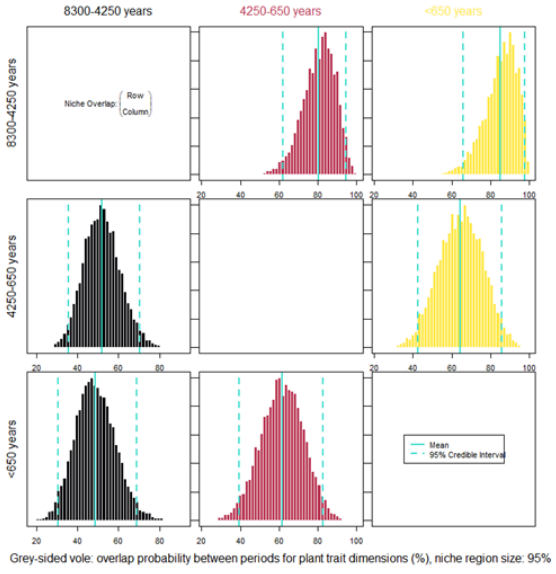

Grey-sided vole: overlap probability between periods for plant trait dimensions (%), niche region size: 95%

681

682

c)

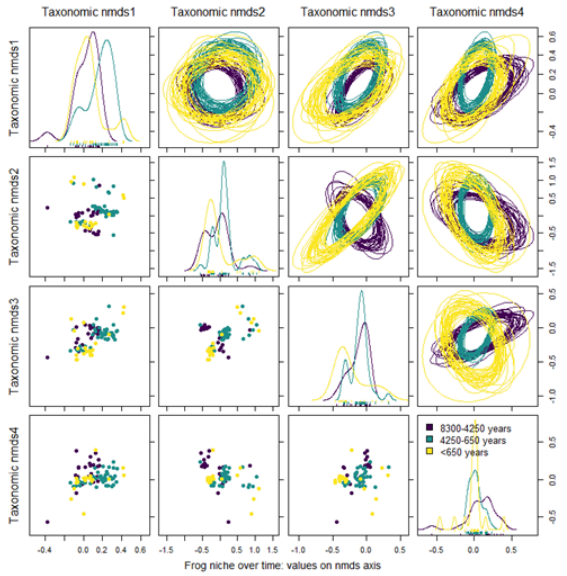

Frog niche over time: values on nmds axis

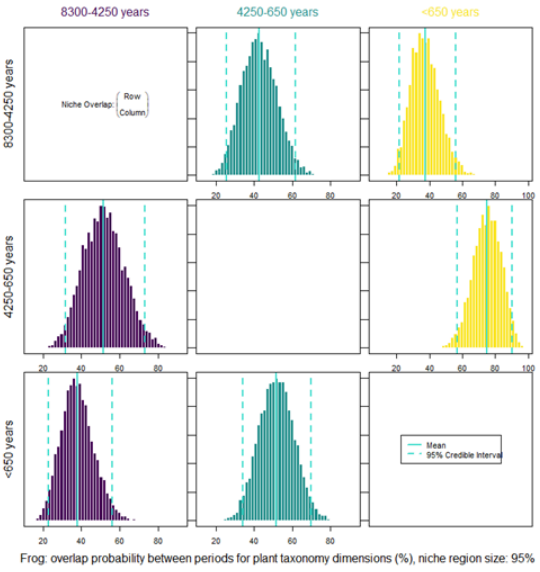

Frog: overlap probability between periods for plant taxonomy dimensions (%), niche region size: 95%

d)

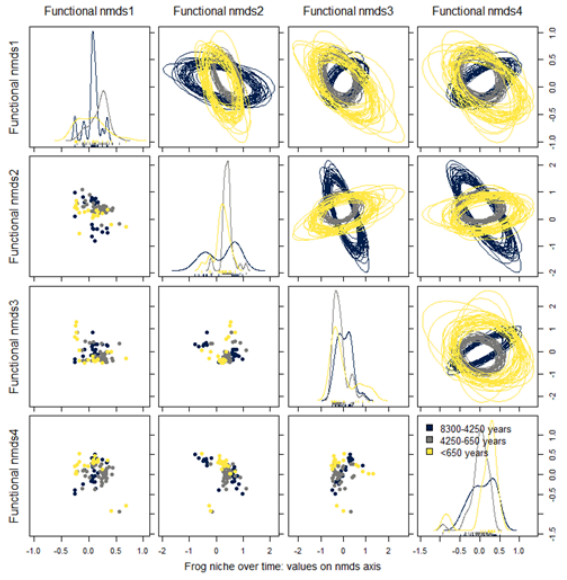

Frog niche over time: values on nmds axis

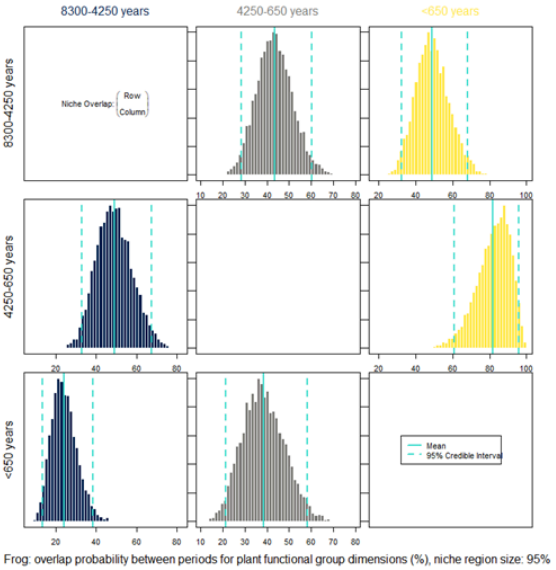

Frog: overlap probability between periods for plant functional group dimensions (%), niche region size: 95%

e)

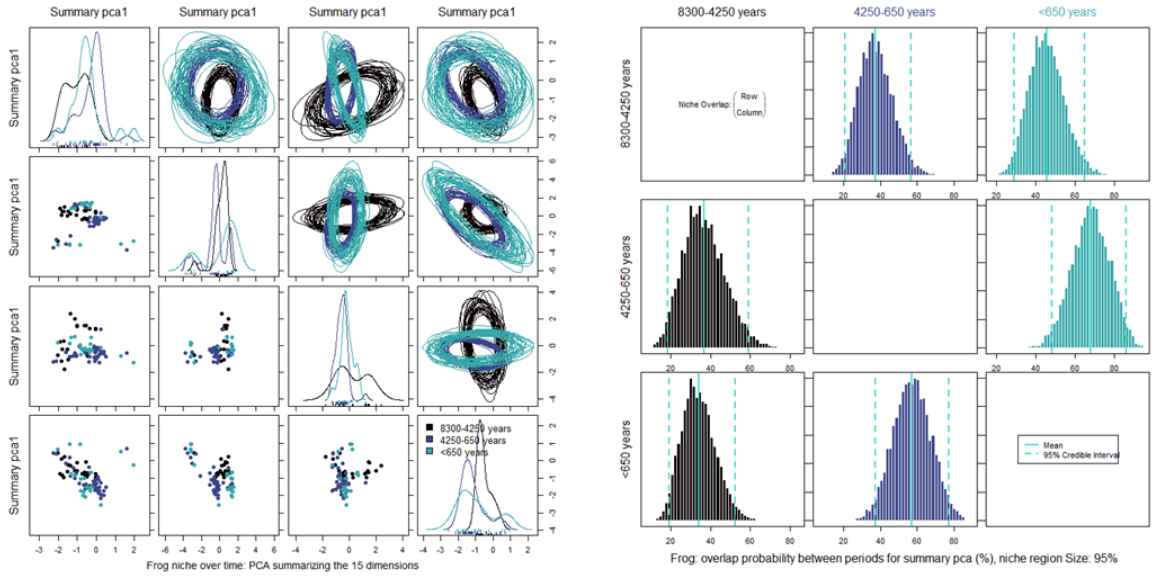

Supplementary Fig. 8.6. Niche stability over time for ***frog*** *(*Rana temporaria*) based on* ***a****, climate niche dimension,* ***b,*** *climate and other abiotic conditions inferred from the traits of plants present,* ***c,*** *vegetation attributes with emphasis on taxonomic richness,* ***d,*** *vegetation attributes using with emphasis on abundance of plant functional composition,* ***e,*** *all 15 niche dimensions summarised using 3 PCA axis representing 70% of the variation. The bar plots represent the posterior probability that an individual from the time period indicated by the row will be found within the niche of the time period indicated by the column header.*

9 Change in environmental space

The environmental space changed over time for all four sets of niche dimensions (Supplementary Fig. 9.1). The climate (mean annual temperature, temperature variability, annual precipitation and mean July temperature) was unstable in the Early and Middle Holocene, and there was also most uncertainty in estimating the climate environmental space in these periods. Climate variability, especially annual precipitation and mean July temperature, narrowed from the Middle Holocene until present. There was less than 50% overlap between the last 650 years and the periods prior to 4.25 ka. The environmental space estimated from abiotic plant traits also showed the largest change between Early and Middle Holocene compared to Late and Historical period, but the overlap in environmental space was higher (70-90% for most comparisons). Thus, in terms of abiotic factors, there was a relatively larger change in climate than in other abiotic factors such as nitrogen, phosphate, pH and light.

The taxonomic richness showed the largest change from a wider taxonomic niche in the Early Holocene that only showed a mean overlap of <30% with later periods. As the peak arrival of plants was around 12 ka [28], the change is likely not due to limited data in the early period but rather represents a shift from a mixture of tundra and boreal habitats to boreal vegetation dominating most sites. In contrast, the plant functional dimensions, which emphasise the abundance of different plant groups, showed higher overlap in niche dimensions and mean probability of overlap of 50% or higher in all cases, probably reflecting that different plant species may fill the same function over time.

When evaluating all 15 niche dimensions, the largest change was between the two earliest time periods compared to the two recent periods (Supplementary Fig. 9.1e). Especially, the probability of finding the environmental space of the Early Holocene was low for the Late Holocene (~38%) and Historical period (~20%), whereas the probability of finding the environmental space of the Middle Holocene in Late Holocene and the Historical period was somewhat higher (40-60%).

a)

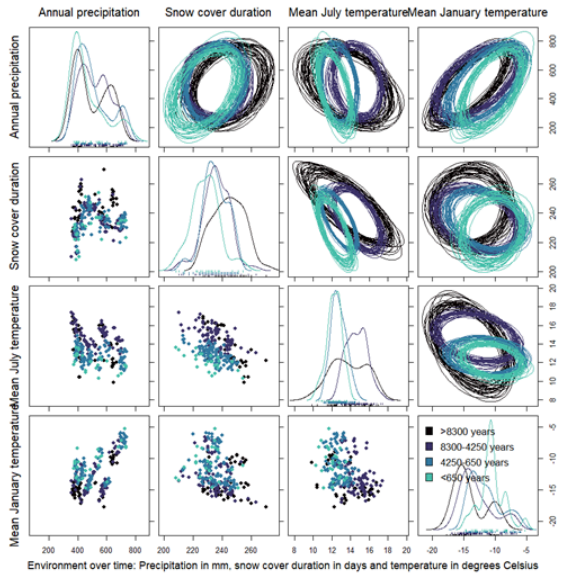

Environment over time: Precipitation in mm, snow cover duration in days and temperature in degrees Celsius

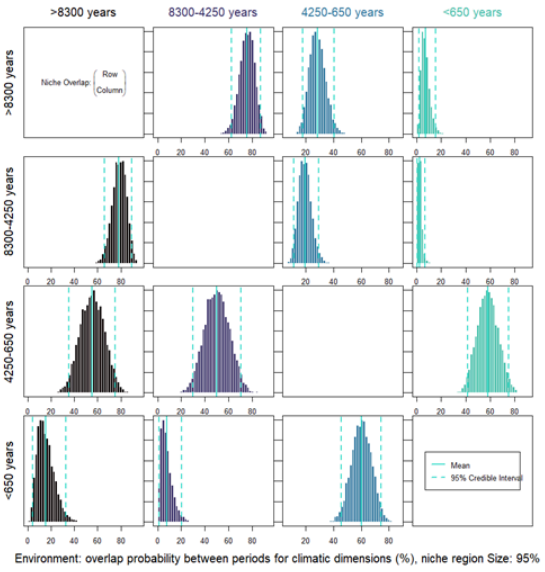

Environment: overlap probability between periods for climatic dimensions (%), niche region Size: 95%

b)

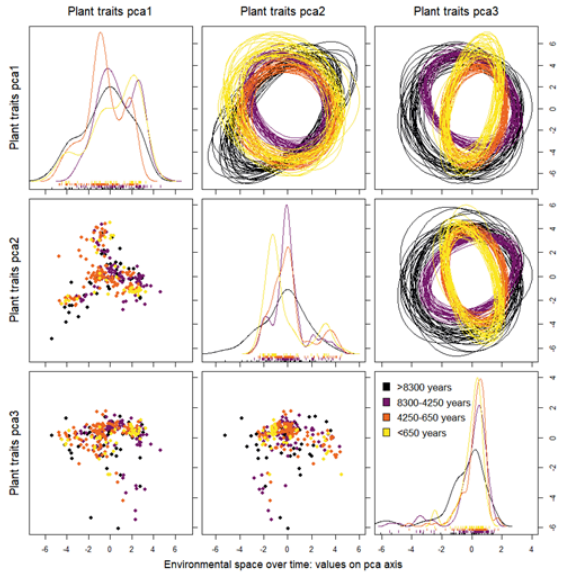

Environmental space over time: values on pca axis

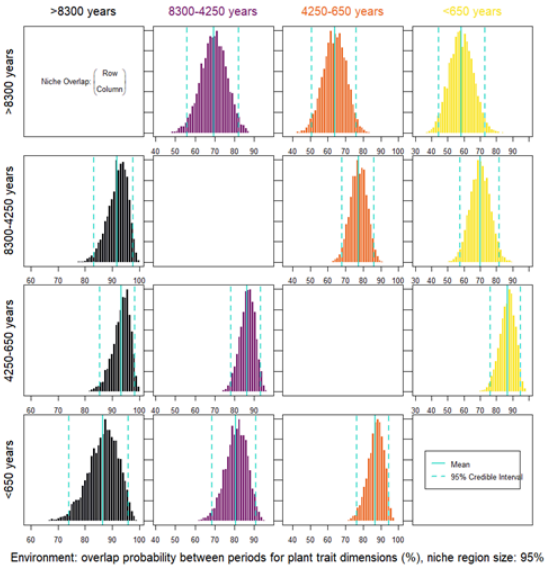

Environment: overlap probability between periods for plant trait dimensions (%), niche region size: 95%

c)

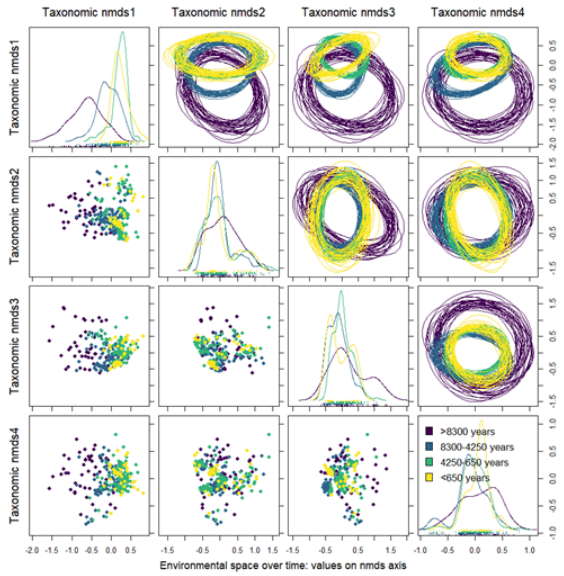
Taxonomic nmds1
Taxonomic nmds2
Taxonomic nmds3
Taxonomic nmds4
>8300 years
8300-4250 years
4250-650 years
<650 years
Environmental space over time: values on nmds axis

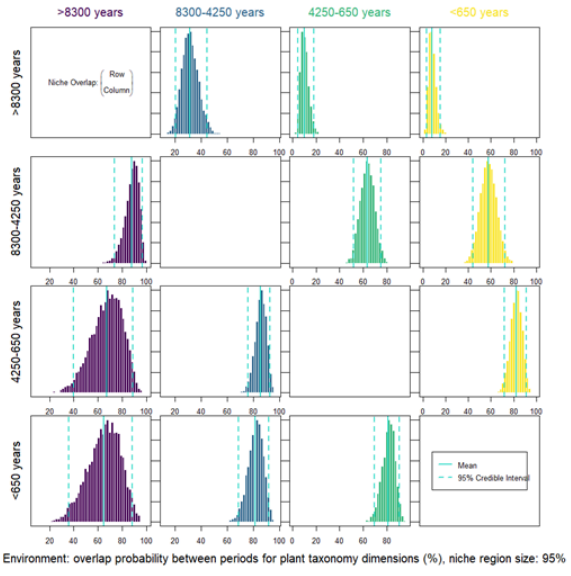
>8300 years
8300-4250 years
4250-650 years
<650 years
Niche Overlap:
Row
Column
Mean
95% Credible Interval
Environment: overlap probability between periods for plant taxonomy dimensions (%), niche region size: 95%

d)

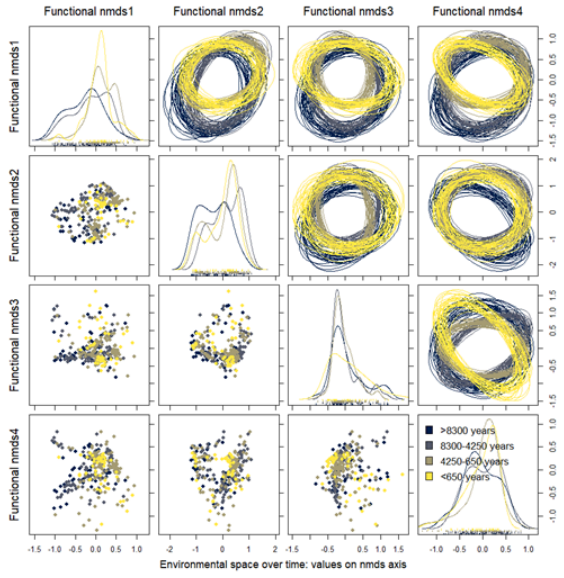
Functional nmds1
Functional nmds2
Functional nmds3
Functional nmds4
>8300 years
8300-4250 years
4250-650 years
<650 years
Environmental space over time: values on nmds axis

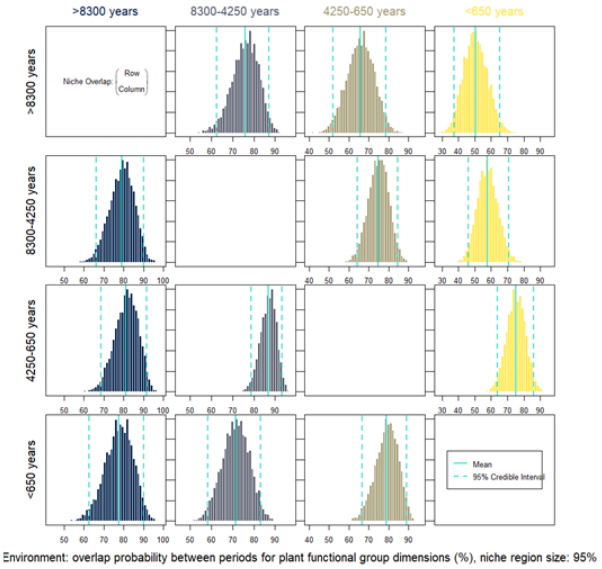
>8300 years
8300-4250 years
4250-650 years
<650 years
Niche Overlap:
Row
Column
Mean
95% Credible Interval
Environment: overlap probability between periods for plant functional group dimensions (%), niche region size: 95%

e)

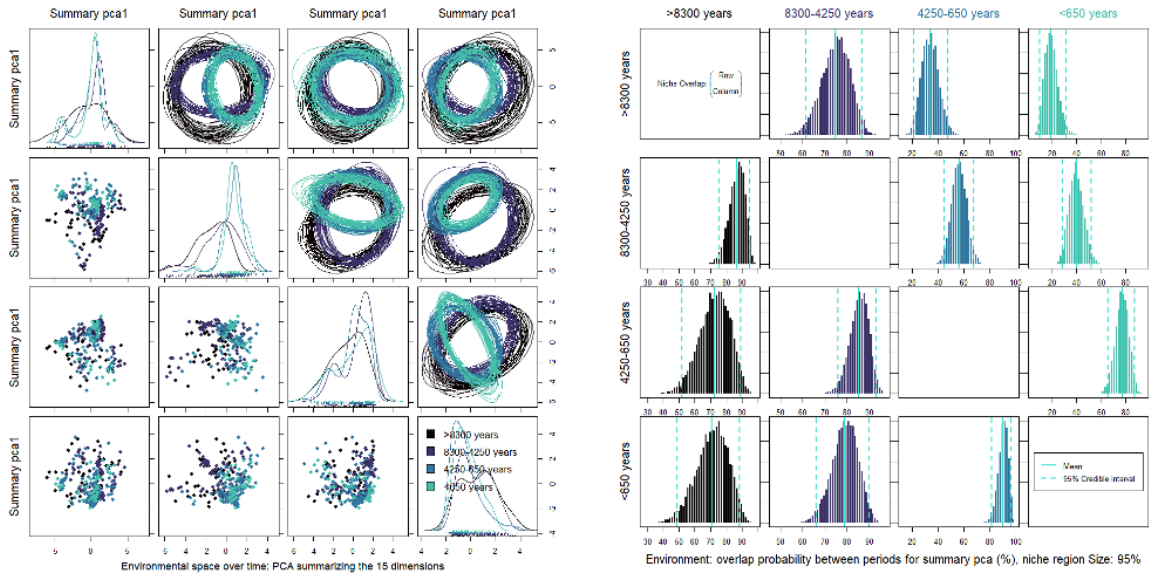

*Supplementary Fig. 9.1. Changes in **environmental space** based on **a**, climate niche dimension, **b,** climate and other abiotic conditions inferred from the traits of plants present, **c,** vegetation attributes with emphasis on taxonomic richness, **d,** vegetation attributes using with emphasis on abundance of plant functional composition, **e,** all 15 niche dimensions summarised using 3 PCA axis representing 70% of the variation. The bar plots represent the posterior probability that ecological conditions from the time period indicated by the row will be found within the time period indicated by the column header.*

10 Niche overlap among key herbivores

For the Middle Holocene, there was a high probability to find willow ptarmigan within the niche of reindeer for the four categories of niche dimensions as well as the combination of all (68-90%, Supplementary Fig. 10.1). There was also a medium high probability to find grey-sided vole in the abiotic niche and functional diversity niche of lemming and reindeer (50-60%), whereas the overlap was otherwise low.

Increasing niche overlap was seen in the Late Holocene where the probability of finding any of the four herbivores within the niche of each of the others were 60-80% for most niche dimensions, and ~90% for finding any of the three others within the abiotic traits and plant taxonomic dimension niche of Norwegian lemming (Supplementary Fig. 10.2). When combining all 15 niche dimensions, there was 70-83% chance to find any of the three other herbivores within the niche of willow ptarmigan, 50-60% to find them within the niche of Norwegian lemming, 58-68% to find them within the niche of reindeer and 80-85% mean probability to find them within the niche of grey-sided vole.

For the Historical period (Supplementary Fig. 10.3), the niche overlap was more complex than in the Late Holocene. The probability to find any of the herbivores within the climatic niche of others was still 60-80% except for a lower probability to find willow ptarmigan and

reindeer within the climatic niche of Norwegian lemming, and a ~90% probability to find any of the smaller herbivores within the climatic niche of reindeer. For abiotic traits, there was a high probability (91-95%) of finding the smaller herbivores within the niche of reindeer, whereas the probability to find reindeer within the smaller niches of Norwegian lemming and grey-sided voles was only 45% and 20%, respectively. For plant taxonomic diversity, the probability of finding reindeer within the niche of any of the smaller herbivores was low (10-25%), in contrast to 80-97% probability of finding the smaller herbivores within the taxonomic niche dimension of reindeer. There was also a low probability of finding willow ptarmigan and Norwegian lemming within the plant taxonomic niche of grey-sided vole, reflecting the overall narrower niche width of grey-sided vole. In contrast, there was a high probability of finding willow ptarmigan and grey-sided vole within the taxonomic niche of lemming. For plant functional groups, there was medium to high overlap among all herbivores (50-92%). When combining all 15 niche dimensions, the probability of finding any of the herbivores within the niche of the smaller herbivores was slightly lower than in the Late Holocene, whereas the probability of finding the smaller herbivores within the niche of reindeer increased from 58-68% in the Late Holocene to 87-92% in the Historical period.

a)

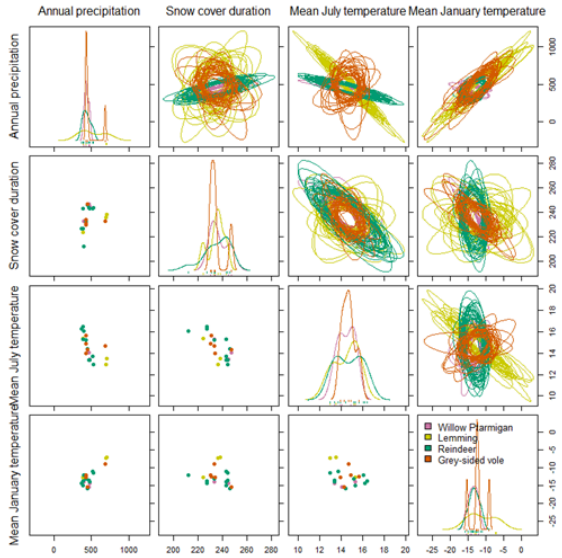

Middle Holocene niche overlap: Precipitation in mm, snow cover duration in days and temperature in degrees Celsius

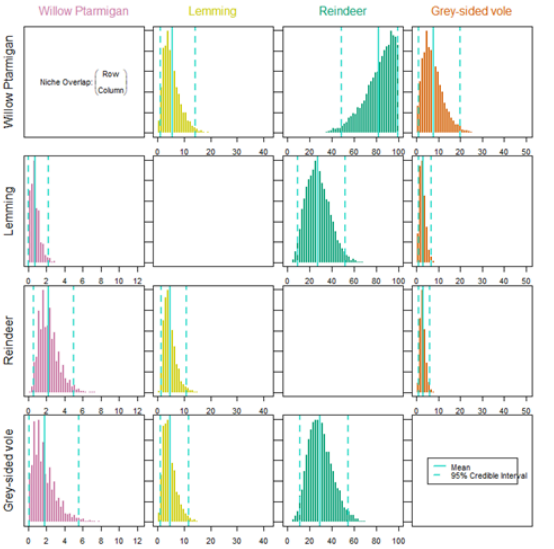

Middle Holocene: overlap probability between periods for climatic dimensions (%), niche region Size: 95%

b)

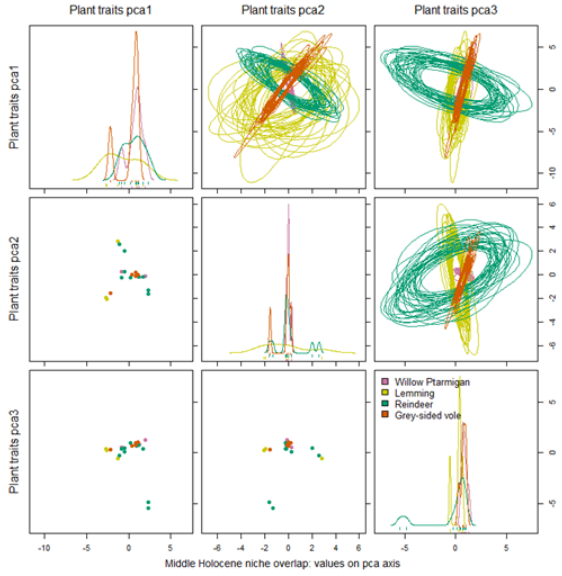

Middle Holocene niche overlap: values on pca axis

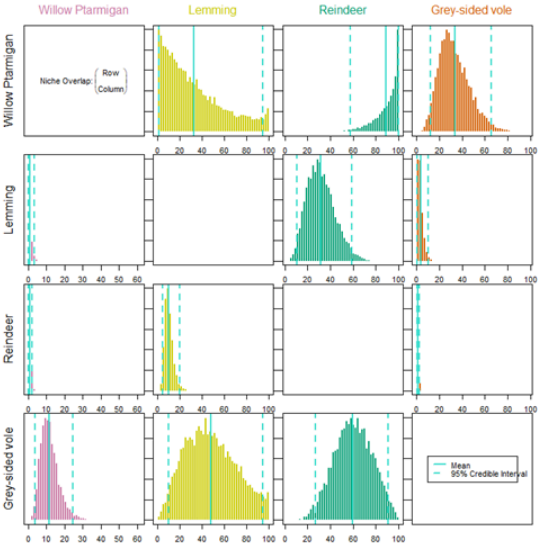

Middle Holocene: overlap probability between periods for plant trait dimensions (%), niche region size: 95%

c)

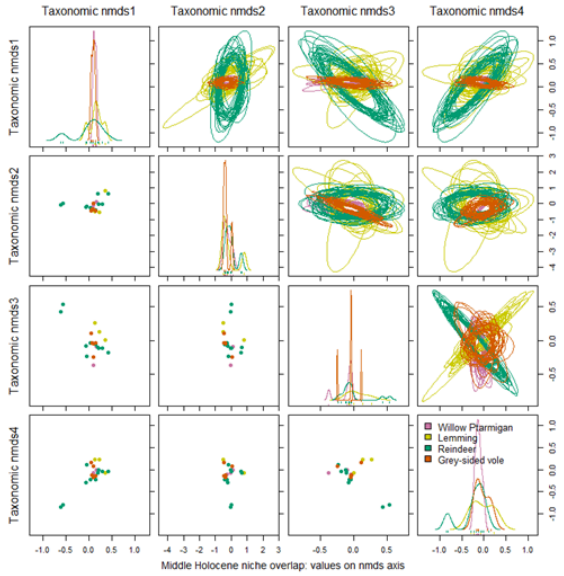
Taxonomic nmds1
Taxonomic nmds2
Taxonomic nmds3
Taxonomic nmds4
Willow Ptarmigan
Lemming
Reindeer
Grey-sided vole
Middle Holocene niche overlap: values on nmds axis

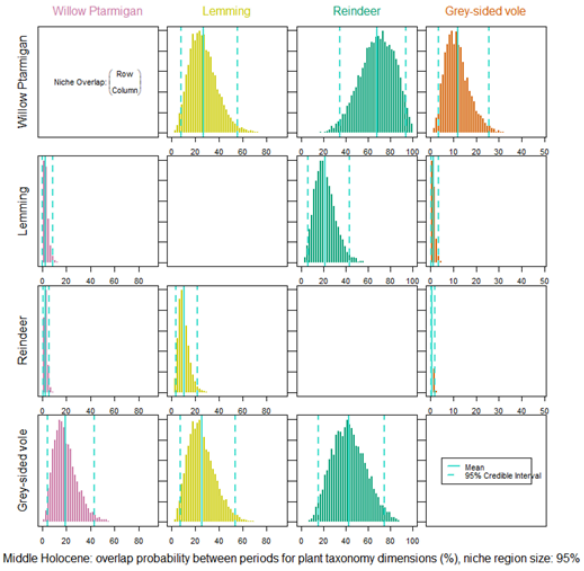
Willow Ptarmigan
Lemming
Reindeer
Grey-sided vole
Niche Overlap:
Row
Column
Mean
95% Credible Interval
Middle Holocene: overlap probability between periods for plant taxonomy dimensions (%), niche region size: 95%

d)

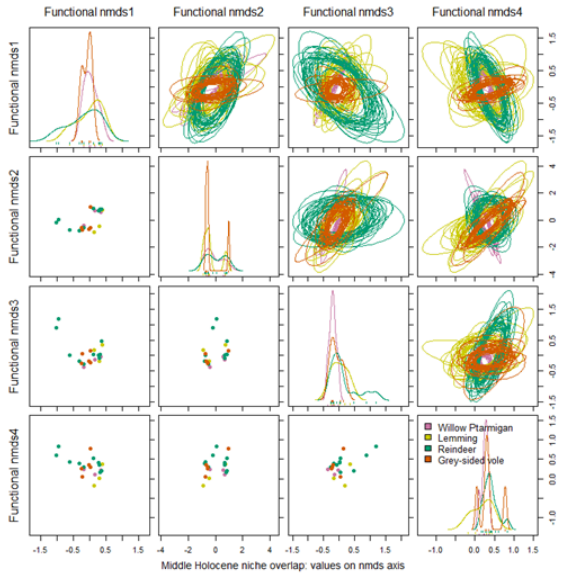
Functional nmds1
Functional nmds2
Functional nmds3
Functional nmds4
Willow Ptarmigan
Lemming
Reindeer
Grey-sided vole
Middle Holocene niche overlap: values on nmds axis

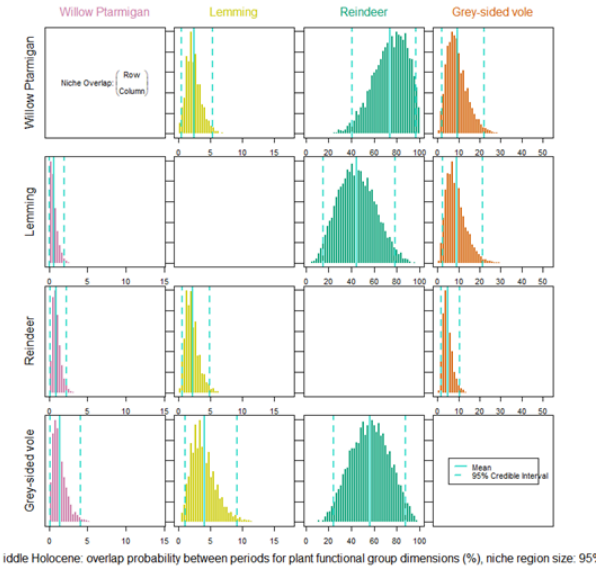
Willow Ptarmigan
Lemming
Reindeer
Grey-sided vole
Niche Overlap:
Row
Column
Mean
95% Credible Interval
iddle Holocene: overlap probability between periods for plant functional group dimensions (%), niche region size: 95

e)

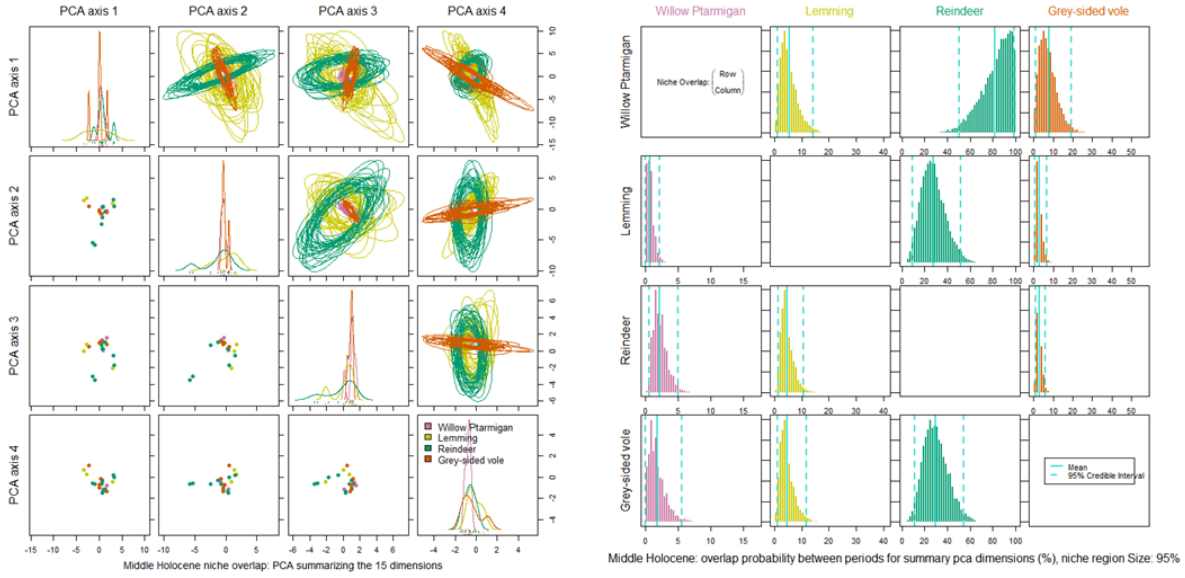

Supplementary Fig. 10.1. ***Niche overlap*** *among key* ***herbivores*** *during* ***Middle Holocene*** *based on* ***a****, climate niche dimension,* ***b,*** *climate and other abiotic conditions inferred from the traits of plants present,* ***c,*** *vegetation attributes with emphasis on taxonomic richness,* ***d,*** *vegetation attributes using with emphasis on abundance of plant functional composition,* ***e,*** *all 15 niche dimensions summarised using 3 PCA axis representing 70% of the variation. The bar plots represent the posterior probability that a species indicated by the row will be found within the niche of the species indicated by the column header.*

a)

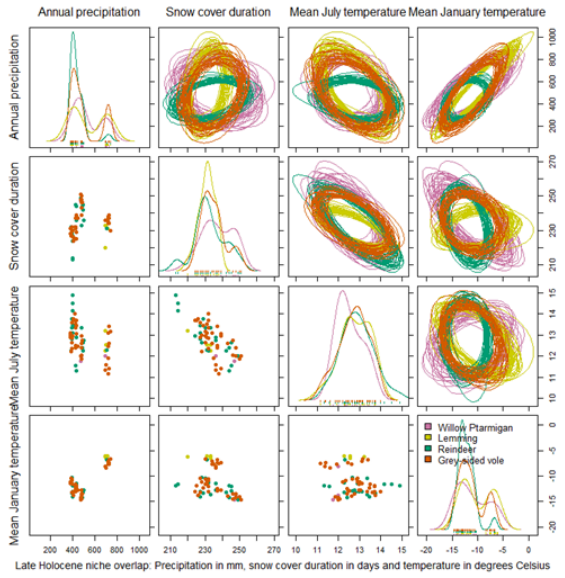

Late Holocene niche overlap: Precipitation in mm, snow cover duration in days and temperature in degrees Celsius

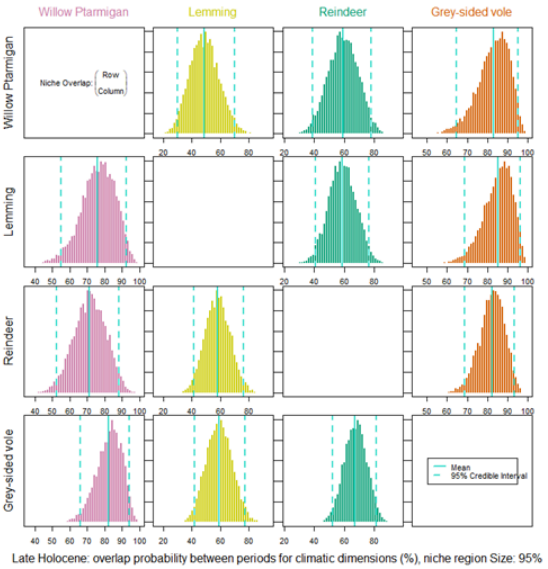

Late Holocene: overlap probability between periods for climatic dimensions (%), niche region Size: 95%

b)

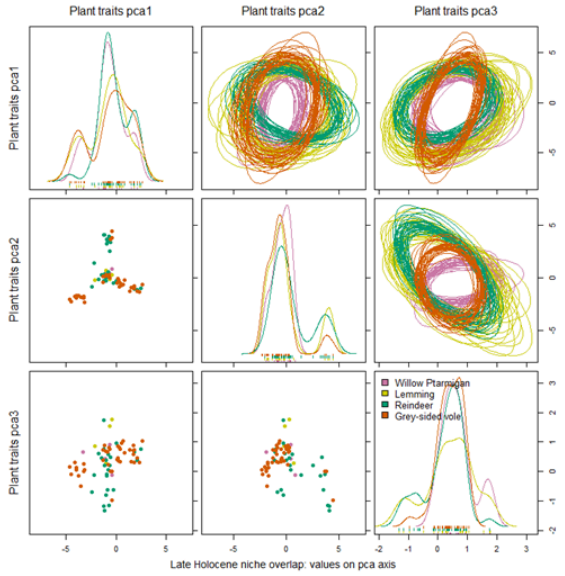

Late Holocene niche overlap: values on pca axis

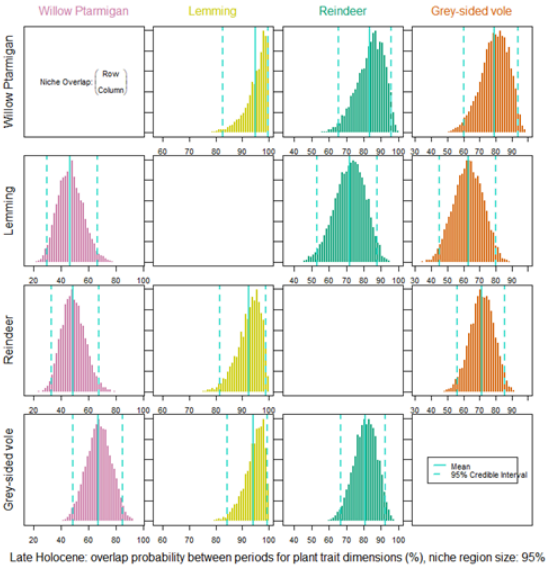

Late Holocene: overlap probability between periods for plant trait dimensions (%), niche region size: 95%

c)

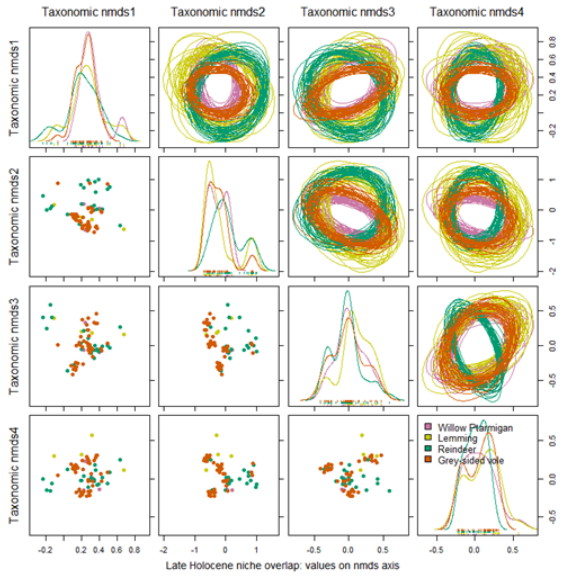

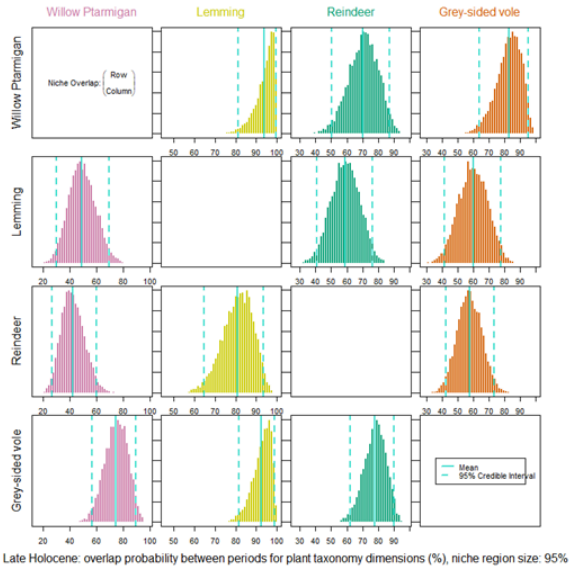

Late Holocene: overlap probability between periods for plant taxonomy dimensions (%), niche region size: 95%

d)

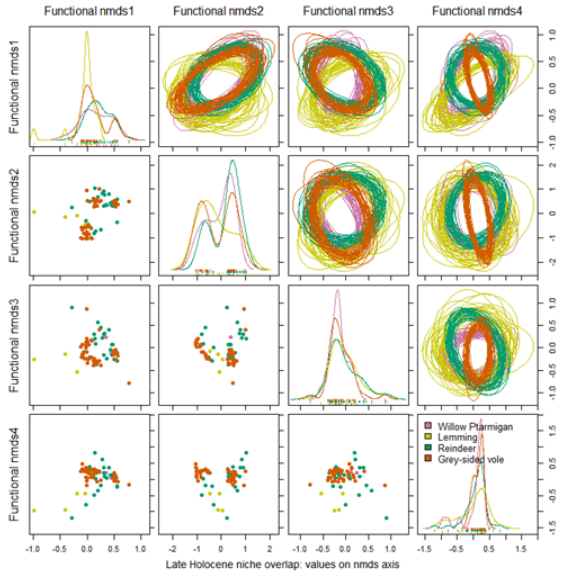

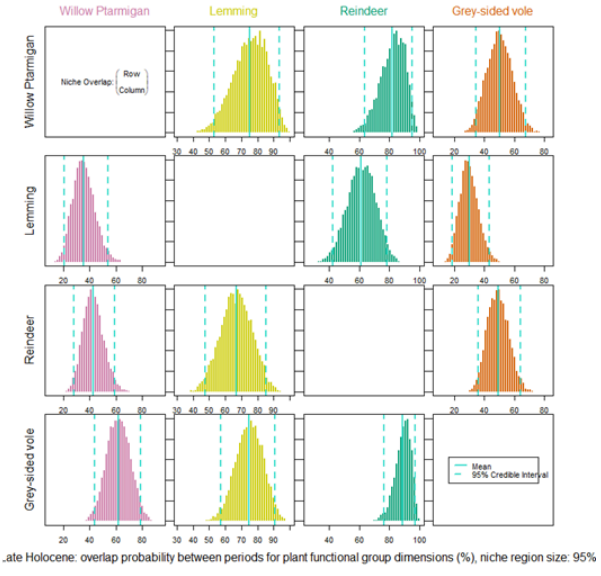

ate Holocene: overlap probability between periods for plant functional group dimensions (%), niche region size: 95%

e)

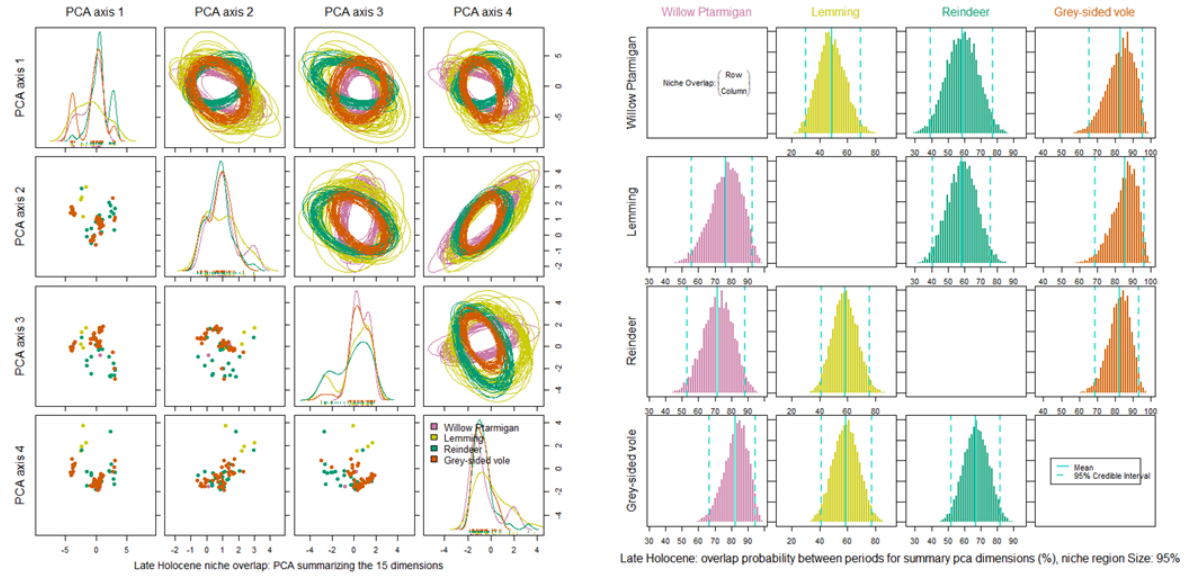

Supplementary Fig. 10.2. ***Niche overlap*** *among key* ***herbivores*** *during* ***Late Holocene*** *based on* ***a****, climate niche dimension,* ***b,*** *climate and other abiotic conditions inferred from the traits of plants present,* ***c,*** *vegetation attributes with emphasis on taxonomic richness,* ***d,*** *vegetation attributes using with emphasis on abundance of plant functional composition,* ***e,*** *all 15 niche dimensions summarised using 3 PCA axis representing 70% of the variation. The bar plots represent the posterior probability that a species indicated by the row will be found within the niche of the species indicated by the column header.*

a)

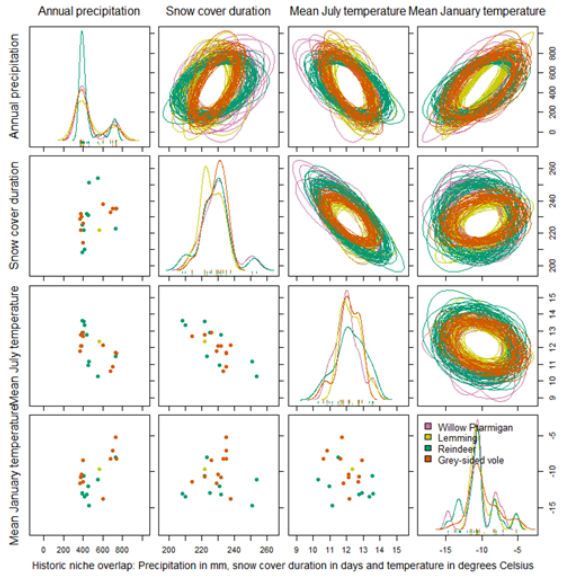
Annual precipitation
Snow cover duration
Mean July temperature
Mean January temperature
Willow Ptarmigan
Lemming
Reindeer
Grey-sided vole
Historic niche overlap: Precipitation in mm, snow cover duration in days and temperature in degrees Celsius

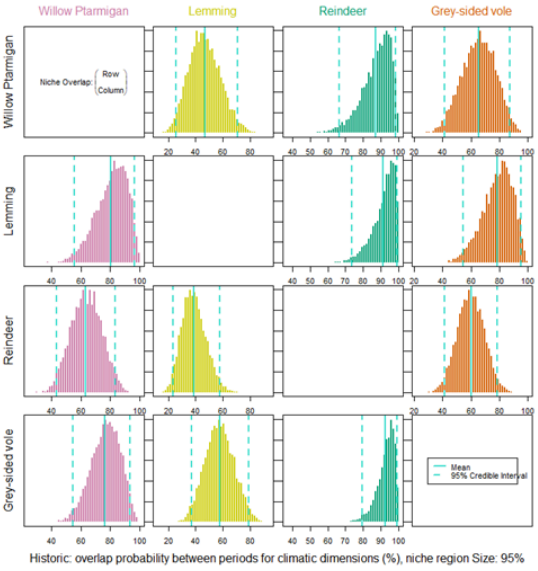
Willow Ptarmigan
Lemming
Reindeer
Grey-sided vole
Niche Overlap:
Row
Column
Mean
95% Credible Interval
Historic: overlap probability between periods for climatic dimensions (%), niche region Size: 95%

b)

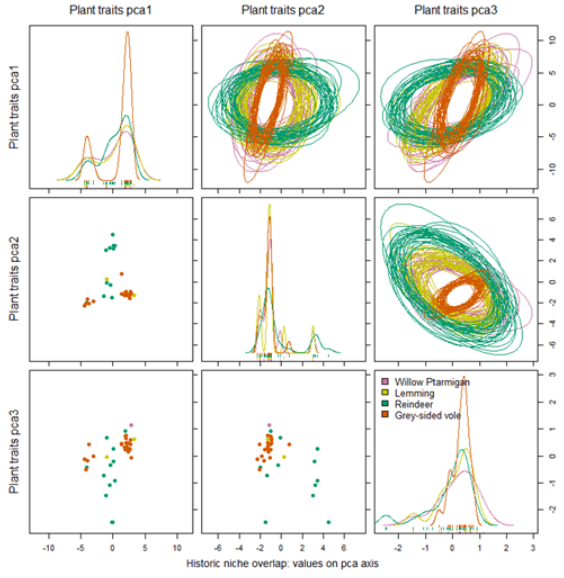
Plant traits pca1
Plant traits pca2
Plant traits pca3
Willow Ptarmigan
Lemming
Reindeer
Grey-sided vole
Historic niche overlap: values on pca axis

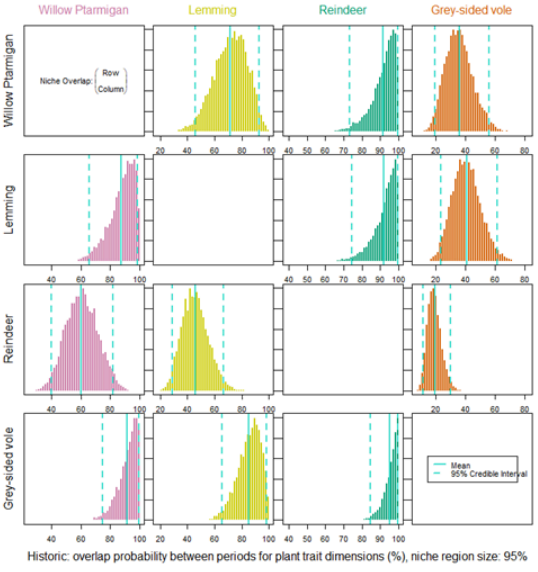
Willow Ptarmigan
Lemming
Reindeer
Grey-sided vole
Niche Overlap:
Row
Column
Mean
95% Credible Interval
Historic: overlap probability between periods for plant trait dimensions (%), niche region size: 95%

c)

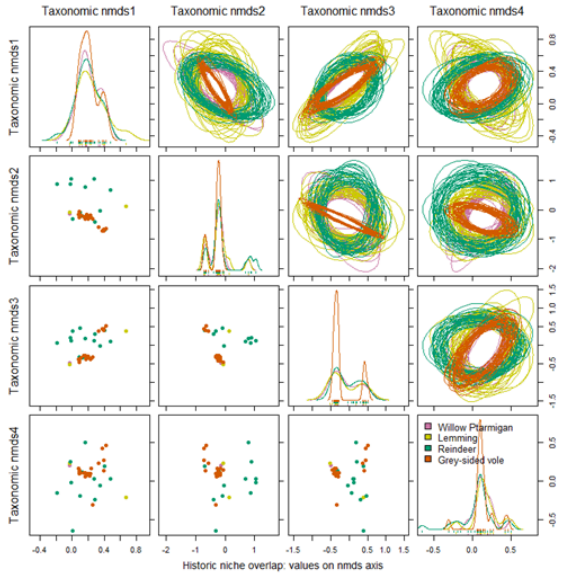
Taxonomic nmds1
Taxonomic nmds2
Taxonomic nmds3
Taxonomic nmds4
Willow Ptarmigan
Lemming
Reindeer
Grey-sided vole
Historic niche overlap: values on nmds axis

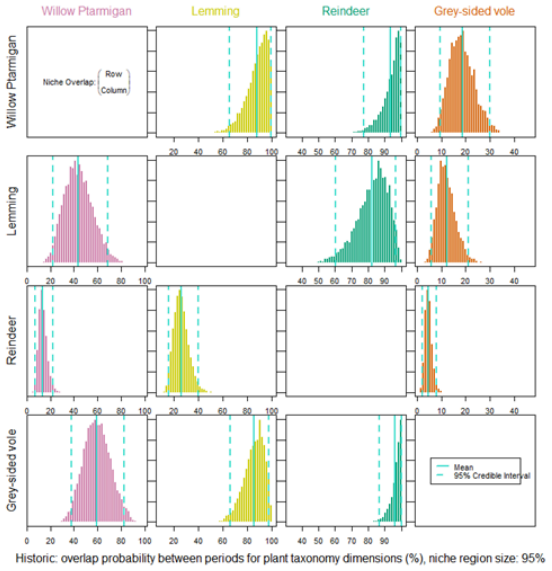
Willow Ptarmigan
Lemming
Reindeer
Grey-sided vole
Niche Overlap:
Row
Column
Mean
95% Credible Interval
Historic: overlap probability between periods for plant taxonomy dimensions (%), niche region size: 95%

d)

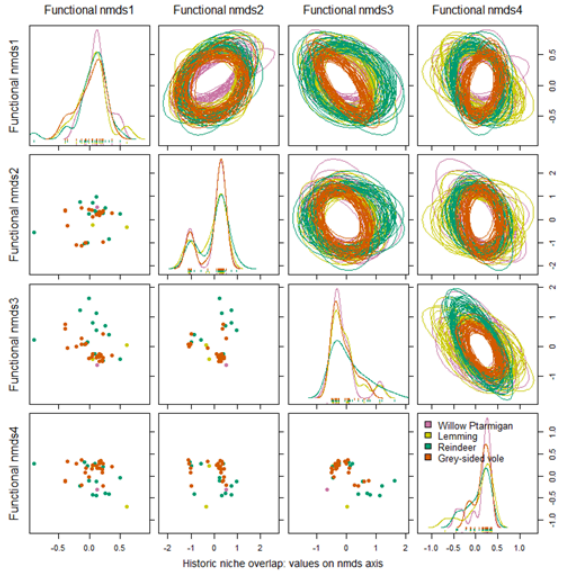
Functional nmds1
Functional nmds2
Functional nmds3
Functional nmds4
Willow Ptarmigan
Lemming
Reindeer
Grey-sided vole
Historic niche overlap: values on nmds axis

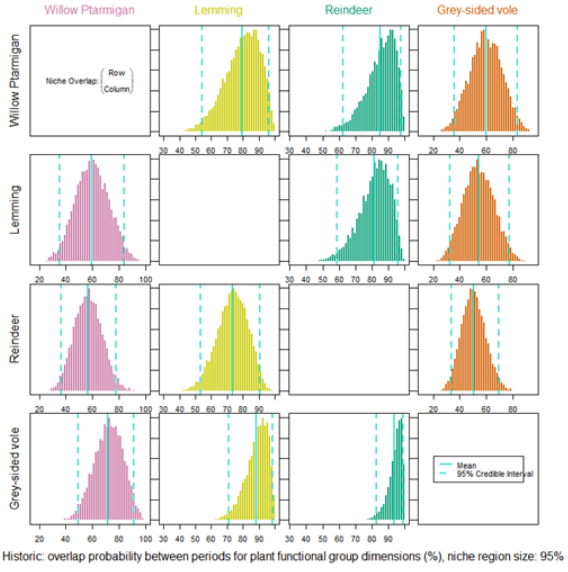
Willow Ptarmigan
Lemming
Reindeer
Grey-sided vole
Niche Overlap:
Row
Column
Mean
95% Credible Interval
Historic: overlap probability between periods for plant functional group dimensions (%), niche region size: 95%

e)

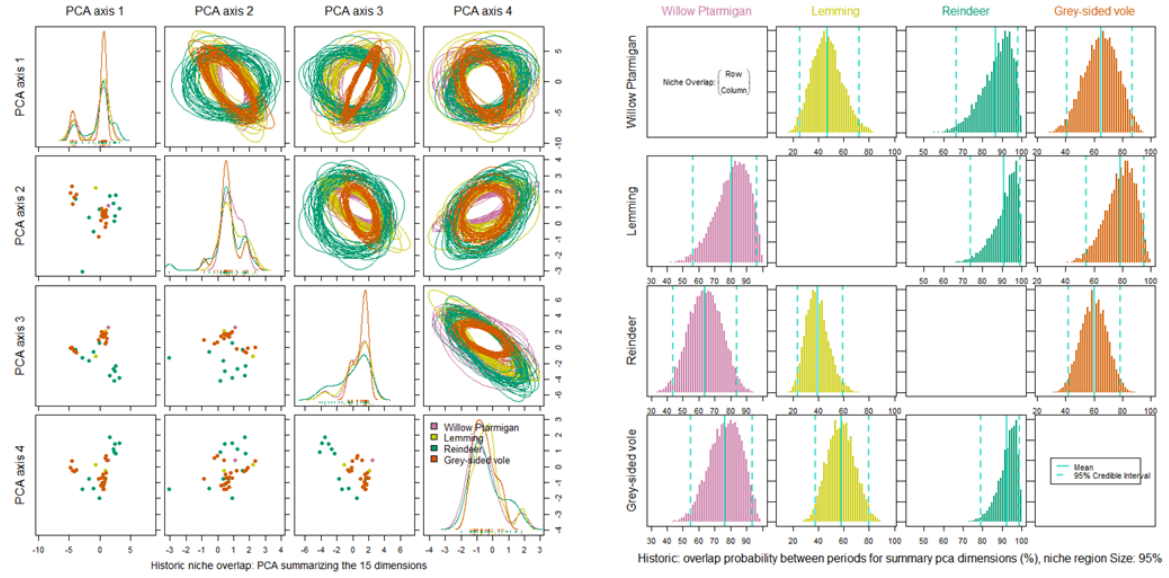

Supplementary Fig. 10.3. ***Niche overlap*** *among key* ***herbivores*** *during* ***Historical*** *time (last 650 years) based on* ***a****, climate niche dimension,* ***b,*** *climate and other abiotic conditions inferred from the traits of plants present,* ***c,*** *vegetation attributes with emphasis on taxonomic richness,* ***d,*** *vegetation attributes using with emphasis on abundance of plant functional composition,* ***e,*** *all 15 niche dimensions summarised using 3 PCA axis representing 70% of the variation. The bar plots represent the posterior probability that a species indicated by the row will be found within the niche of the species indicated by the column header.*

11 Lemming and tundra vole 16S reference sequences

We supplemented our EMBL-derived animal 16S reference library with three sequences from Norwegian lemming (*Lemmus lemmus*), Siberian lemming (*Lemmus sibiricus*), and tundra vole (*Microtus oeconomus*). The Norwegian lemming sequence was previously presented in [52], whereas the Siberian lemming sequence was provided by David Díez del Molino and Love Dalén (Swedish Museum of Natural History/Stockholm University, Sweden).

Although a genome assembly is available for the tundra vole (NCBI RefSeq GCA_007455595.1), the mitochondrial genome is not included. We therefore searched the underlying raw sequence data used to generate this genome (NCBI BioProject PRJNA551187) to extract a tundra vole 16S sequence for use in the reference library. To do this, we grep-searched the raw sequence data for both the forward and reverse 16S P007 primer sequences [53] in both the forward and reverse complement orientations (for four searches in total). We then compiled the recovered reads and converted them to the same orientation. The reads were converted to FASTA format, aligned using the clustal algorithm [54] in SeaView v4 [55], and a 90% majority-rule consensus sequence was generated in SeaView. Due to the short length of the barcode, this strategy allowed for the complete reconstruction

of the targeted 16S region. The consensus sequence was then trimmed to the barcode coordinates and the reconstructed barcode underwent an NCBI BLAST search against PRJNA551187, which had multiple 100% matches. Since this reference sequence was generated, a further three tundra vole 16S sequences are now available on NCBI Genbank (ON165388, ON165345, ON165278), which altogether have seven variable positions, of which only one is unique to the sequence presented here. Altogether, these checks demonstrate the validity of the reconstructed tundra vole 16S sequence used in our reference library.

The three reference sequences used to supplement the reference library were:

>Lemmus_lemmus_16S_P007
TTAATTTCCTGGCCTAACTTATAAACTTATACCTCTACTGAACTAAATAGTAAAGTCATAGG
CTAGCAATTTC
>Lemmus_sibiricus_16S_P007
TTAATTTCCTGGCCTAACTTATAAACCTATACCTCTACTGAACTAAACAATAAAGTCATAGG
CTAGCAATTTC
>Microtus_oeconomus_16S_P007_reconstructed
TTAATTTCCTAGCTTAGCTACCCAACTTACTCCCCTACGGGACCAAAAAGAAAAGAAATAA
GCTAGTAATTTC

Supplementary references

1. Hughes, A. L. C., Gyllencreutz, R., Lohne, Ø. S., Mangerud, J. & Svendsen, J. I. The last Eurasian ice sheets – a chronological database and time-slice reconstruction, DATED-1. *Boreas* **45**, 1–45 (2016).
2. Patton, H. *et al.* Deglaciation of the Eurasian ice sheet complex. *Quat. Sci. Rev.* **169**, 148–172 (2017).
3. Påsse, T. & Andersson, L. Shore-level displacement in Fennoscandia calculated from empirical data. *GFF* **127**, 253–268 (2005).
4. Corner, G. D., Yevzerov, V. Y., Kolka, V. V. & Møller, J. J. Isolation basin stratigraphy and Holocene relative sea-level change at the Norwegian—Russian border north of Nikel, northwest Russia. *Boreas* **28**, 146–166 (1999).
5. Stepanova, A. *et al.* Late Weichselian to Holocene history of the Baltic Sea as reflected in ostracod assemblages. *Boreas* **48**, 761–778 (2019).
6. Bradley, S. L., Ely, J. C., Clark, C. D., Edwards, R. J. & Shennan, I. Reconstruction of the palaeo-sea level of Britain and Ireland arising from empirical constraints of ice extent: implications for regional sea level forecasts and North American ice sheet volume. *J. Quat. Sci.* **38**, 791–805 (2023).
7. Giguet-Covex, C., Jelavić, S. & Foucher, A. The Sources and Fates of Lake Sedimentary DNA. *Change Using Lake …* (2023).
8. Ataman, T. G., Lammers, Y., Alsos, I. G., Rijal, D. P. & Brown, A. G. Sedimentary DNA from lake depocenters maximizes detection of catchment vegetation. *Commun. Earth Environ.* **6**, 1–10 (2025).
9. Brown, A. G. *et al.* New integrated molecular approaches for investigating lake settlements in north-western Europe. *Antiquity* **96**, 1179–1199 (2022).

10. Picard, M. *et al.* Using DNA archived in lake sediments to reconstruct past ecosystems. in *Encyclopedia of Quaternary Science* 673–690 (Elsevier, 2025).
11. Pedersen, M. W. *et al.* Ancient and modern environmental DNA. *Philosophical Transactions of the Royal Society of London Series B-Biological Sciences* **370**, 20130383 (2015).
12. Sand, K. K., Jelavić, S., Kjær, K. H. & Prohaska, A. Importance of eDNA taphonomy and sediment provenance for robust ecological inference: Insights from interfacial geochemistry. *Environ. DNA* **6**, (2024).
13. Alvarez, A. J., Khanna, M., Toranzos, G. A. & Stotzky, G. Amplification of DNA bound on clay minerals. *Mol. Ecol.* **7**, 775–778 (1998).
14. Kjær, K. H. *et al.* A 2-million-year-old ecosystem in Greenland uncovered by environmental DNA. *Nature* **612**, 283–291 (2022).
15. Deiner, K., Fronhofer, E. A., Mächler, E., Walser, J.-C. & Altermatt, F. Environmental DNA reveals that rivers are conveyer belts of biodiversity information. *Nat. Commun.* **7**, 12544 (2016).
16. Hardeng, J., Bakke, J., Sabatier, P., Støren, E. W. N. & Van der Bilt, W. Lake sediments from southern Norway capture Holocene variations in flood seasonality. *Quat. Sci. Rev.* **290**, 107643 (2022).
17. Morlock, M. A., Rodriguez-Martinez, S., Huang, D. Y.-T. & Klaminder, J. Erosion regime controls sediment environmental DNA-based community reconstruction. *Environ. DNA* **5**, 1393–1404 (2023).
18. Sjögren, P. *et al.* Lake sedimentary DNA accurately records 20th Century introductions of exotic conifers in Scotland. *New Phytol.* **213**, 929–941 (2017).
19. Ficetola, G. F. *et al.* DNA from lake sediments reveals long-term ecosystem changes after a biological invasion. *Sci. Adv.* **4**, eaar4292 (2018).
20. Giguet-Covex, C. *et al.* New insights on lake sediment DNA from the catchment: importance of taphonomic and analytical issues on the record quality. *Sci. Rep.* **9**, 14676 (2019).

21. Salonen, J. S. *et al.* Uncovering Holocene climate fluctuations and ancient conifer populations: Insights from a high-resolution multi-proxy record from Northern Finland. *Glob. Planet. Change* **237**, 104462 (2024).
22. Rijal, D. P. *et al.* Sedimentary ancient DNA shows terrestrial plant richness continuously increased over the Holocene in northern Fennoscandia. *Science Advances* **7**, eabf9557 (2021).
23. Brown, A. G., Lucas, M., Alsos, I. G., Fromm, B. & Hudson, S. The sedaDNA revolution and archaeology: Progress, challenges, and a research agenda. *J. Archaeol. Sci.* **174**, 106132 (2025).
24. Capo, E. *et al.* Lake Sedimentary DNA Research on Past Terrestrial and Aquatic Biodiversity: Overview and Recommendations. *Quaternary* **4**, 6 (2021).
25. Liu, S. *et al.* Sedimentary ancient DNA reveals a threat of warming-induced alpine habitat loss to Tibetan Plateau plant diversity. *Nat. Commun.* **12**, 2995 (2021).
26. Liu, Y., Lisovski, S., Courtin, J., Stoof-Leichsenring, K. R. & Herzschuh, U. Plant interactions associated with a directional shift in the richness range size relationship during the Glacial-Holocene transition in the Arctic. *Nat. Commun.* **16**, 1128 (2025).
27. Garcés-Pastor, S. *et al.* Wild and domesticated animal abundance is associated with greater late-Holocene alpine plant diversity. *Nat. Commun.* **16**, 3924 (2025).
28. Alsos, I. G. *et al.* Postglacial species arrival and diversity buildup of northern ecosystems took millennia. *Science Advances* **8**, eabo7434 (2022).
29. Nesje, A. A piston corer for lacustrine and marine sediments. *Arct. Alp. Res.* **24**, 257–259 (1992).
30. Garcés-Pastor, S. *et al.* Terrestrial Plant DNA from Lake Sediments: Volume 6: Sedimentary DNA. in *Tracking Environmental Change Using Lake Sediments* (eds. Capo, E., Barouillet, C. & Smol, J. P.) vol. 21 275–298 (Springer International Publishing, Cham, 2023).
31. Leonard, J. A. *et al.* Animal DNA in PCR reagents plagues ancient DNA research. *J. Archaeol. Sci.* **34**, 1361–1366 (2007).

32. Wang, Y. *et al.* Late Quaternary dynamics of Arctic biota from ancient environmental genomics. *Nature* (2021) doi:10.1038/s41586-021-04016-x.
33. Renaud, G., Schubert, M., Sawyer, S. & Orlando, L. Authentication and assessment of contamination in ancient DNA. *Methods Mol. Biol.* **1963**, 163–194 (2019).
34. Heintzman, P. D. *et al.* The Sedimentary Ancient DNA Workflow. in *Tracking Environmental Change Using Lake Sediments* (ed. Eric Capo, Cécilia Barouillet, John P. Smol) 53–84 (Springer Nature, Cham, Switzerland, 2023).
35. Schnell, I. B., Bohmann, K. & Gilbert, M. T. P. Tag jumps illuminated – reducing sequence-to-sample misidentifications in metabarcoding studies. *Mol. Ecol. Resour.* **15**, 1289–1303 (2015).
36. Valen, V., Mangerud, J., Larsen, E. & Hufthammer, A. K. Sedimentology and stratigraphy in the cave Hamnsundhelleren, western Norway. *J. Quat. Sci.* **11**, 185–201 (1996).
37. Bachura, O. P. & Kosintsev, P. A. Holocene Large Mammal Fauna of the Central Part of the East European Plain. *Biology Bulletin* **47**, 996–1012 (2020).
38. Salmi, A.-K., van den Berg, M., Niinimäki, S. & Pelletier, M. Earliest archaeological evidence for domesticated reindeer economy among the Sámi of Northeastern Fennoscandia AD 1300 onwards. *J. Anthropol. Archaeol.* **62**, 101303 (2021).
39. Bråthen, K. A. *et al.* Endozoochory varies with ecological scale and context. *Ecography* **30**, 308–320 (2007).
40. Steinthorsdottir, L. Investigating trophic interactions among herbivorous species in a rapidly changing Arctic tundra usingDNA metabarcoding. (University of Oslo, 2019).
41. Soininen, E. M. *et al.* Not only mosses: lemming winter diets as described by DNA metabarcoding. *Polar Biol.* **40**, 2097–2103 (2017).
42. Soininen, E. M. *et al.* Shedding new light on the diet of Norwegian lemmings: DNA metabarcoding of stomach content. *Polar Biol.* **36**, 1069–1076 (2013).
43. Unander, S., Mortensen, A. & Elvebakk, A. Seasonal changes in crop content of the Svalbard Ptarmigan *Lagopus mutus hyperboreus*. *Polar Res.* **3**, 239–245 (1985).

44. Ingvaldsen, E. W. *et al.* Fecal DNA metabarcoding reveals seasonal and annual variation in willow ptarmigan diet. *R. Soc. Open Sci.* **11**, 231518 (2024).
45. Garcés-Pastor, S. *et al.* High resolution ancient sedimentary DNA shows that alpine plant diversity is associated with human land use and climate change. *Nat. Commun.* **13**, 1–16 (2022).
46. Barbero-Palacios, L. *et al.* Herbivore diversity effects on Arctic tundra ecosystems: a systematic review. *Environ. Evid.* **13**, 6 (2024).
47. Kamenova, S. *et al.* Arctic greening drives changes in the diet and gut microbiome of a resident herbivore with consequences for fitness. *bioRxiv* 2024.02.27.582426 (2024) doi:10.1101/2024.02.27.582426.
48. Trondrud, L. M. *et al.* A summer heat wave reduced activity, heart rate, and autumn body mass in a cold-adapted ungulate. *Physiol. Biochem. Zool.* **96**, 282–293 (2023).
49. Stark, S. *et al.* The ecosystem effects of reindeer (Rangifer tarandus) in northern Fennoscandia: Past, present and future. *Perspect. Plant Ecol. Evol. Syst.* **58**, 125716 (2023).
50. Ims, R. A. *et al.* Can reindeer overabundance cause a trophic cascade? *Ecosystems* **10**, 607–622 (2007).
51. Johnson, R. K. & Toprak, V. Local habitat is a strong determinant of spatial and temporal patterns of macrophyte diversity and composition in boreal lakes. *Freshw. Biol.* **66**, 1490–1501 (2021).
52. Brown, T. *et al.* Paleoeconomy more than demography determined prehistoric human impact in Arctic Norway. *PNAS Nexus* **1**, gac209 (2022).
53. Giguet-Covex, C. *et al.* Long livestock farming history and human landscape shaping revealed by lake sediment DNA. *Nat. Commun.* **5**, (2014).
54. Sievers, F. *et al.* Fast, scalable generation of high-quality protein multiple sequence alignments using Clustal Omega. *Mol. Syst. Biol.* **7**, 539 (2011).
55. Gouy, M., Guindon, S. & Gascuel, O. SeaView version 4: A multiplatform graphical user interface for sequence alignment and phylogenetic tree building. *Mol. Biol. Evol.* **27**,

221–224 (2010).